SVERIGES GEOLOGISKA UNDERSÖKNING

SERIE C NR 734 AVHANDLINGAR OCH UPPSATSER ÅRSBOK 71 NR 9

ANDERS CARLSSON AND TOMMY OLSSON

WATER LEAKAGE IN THE FORSMARK TUNNEL, UPPLAND, SWEDEN

STOCKHOLM 1977

SGU C 734 • ANDERS CARLSSON AND TOMMY OLSSON: Water leakage in the Forsmark Tunnel, Uppland, Sweden

SERIE C NR 734 AVHANDLINGAR OCH UPPSATSER ÅRSBOK 71 NR 9

ANDERS CARLSSON AND TOMMY OLSSON

WATER LEAKAGE IN THE FORSMARK TUNNEL, UPPLAND, SWEDEN

STOCKHOLM 1977

Addresses:

Anders Carlsson
Swedish State Power Board
Civil Engineering Development
Department of Engineering Geology
S-162 87 VÄLLINGBY, Sweden

Tommy Olsson
Geological Survey of Sweden
Department of Quaternary Geology and Hydrogeology
Box 2048, S-183 02 TÄBY, Sweden

Kartan på s. 4 är godkänd ur sekretessynpunkt för spridning.
Statens Lantmäteriverk 1977-02-10.

Schmidts Boktryckeri AB
Helsingborg 1977

CONTENTS

ABSTRACT

During the geological mapping of the Forsmark tunnel, special attention was given to observing and recording the occurrence and volume of groundwater inflow.

The purpose of this work was, in the first place, to substantiate the occurrence and the volume of the water leakages in relation to the predominant geological and tectonic conditions. In the second place, its purpose was to show the different water storages in the rock mass, their mutual relationships and their communication with the sea-water reservoir with regard to the water-bearing capacity.

On the basis of the results of the geological explorations, we have tried to calculate the volume of the water leakages and the variations of the leak intensity along the tunnel line. The result of the calculation has been compared with and judged by the results of the geological survey in the tunnel.

INTRODUCTION

The Forsmark nuclear-power plant is situated on the east coast of Sweden in the north-eastern part of the county of Uppland. The first stage of construction includes two power-units with a discharge tunnel for the cooling water. This tunnel has a total length of about 2300 m and runs from the station area via a surge basin to discharge at Loven Island into an artificial "biotest lake". In this paper, we discuss the groundwater leakage into the 1921-m-long section between the surge basin and the outlet (Fig. 1).

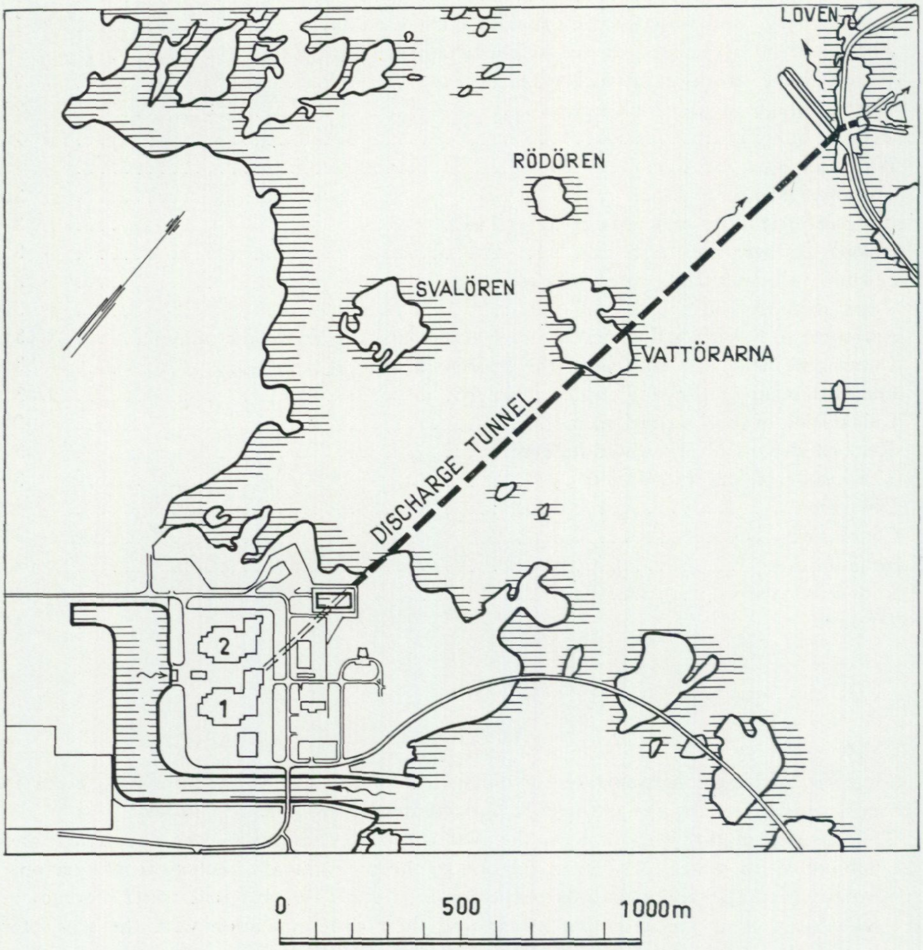

Fig. 1. Plan of the Forsmark area. The figures 1 and 2 represent Unit 1 and Unit 2 respectively. The part of the Forsmark tunnel investigated is indicated by the the broken line.
Plan över Forsmarksområdet. Siffrorna 1 och 2 representerar block 1 och 2. Den undersökta delen av Forsmarktunneln är markerad av den streckade linjen.

When the two power-units are in operation, heated cooling water will flow at a rate of 87 m^3/s from the power station into the sea. The temperature of the cooling water will be about 10°C higher than that of the sea water.

The cross sectional area of the tunnel is about 80 m^2, with a top-heading of about 50 m^2 and a bench of about 30 m^2. The dimensions of the top heading are shown in Fig. 2. The tunnel is about 75 m below sea level, the rock cover being approximately 55–60 m thick. The construction of the discharge tunnel was started in 1974 and finished in 1976.

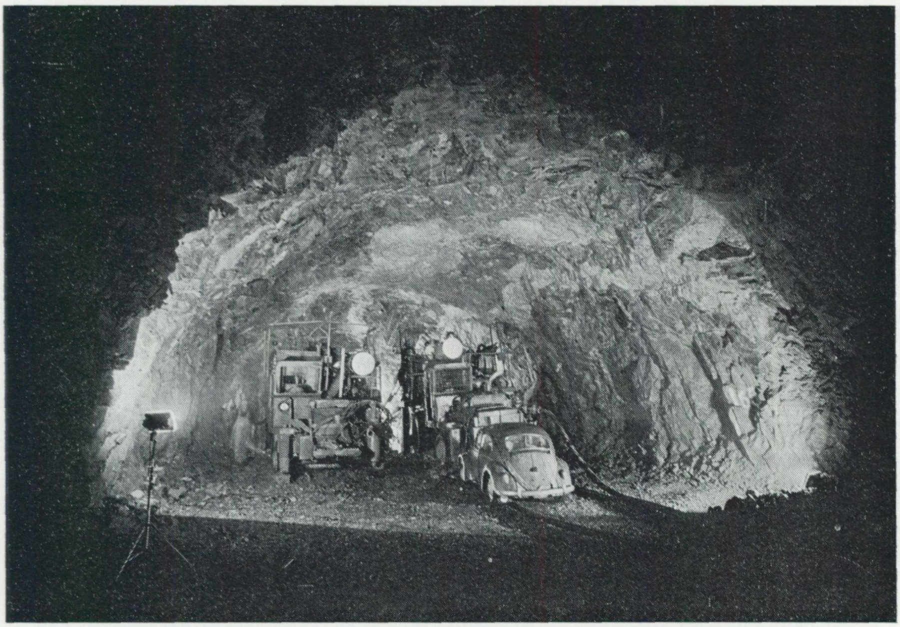

Fig. 2. Cross-section of the top heading of the tunnel. (Photograph by G. Hansson.)
Tvärsnitt av tunnels takort.

As shown in Fig. 1 and Fig. 3, for most of its length the discharge tunnel runs underneath the Gulf of Bothnia. Consequently, the rocks along the tunnel site have an unlimited infiltration reservoir close at hand. The sea acts as an infiltration reservoir with a constant head pressure which has simplified observations of the water storages in the rock mass and the drainage effect of the tunnel.

The purpose of this work, in the first place, was to substantiate the occurrence and the volume of the water leakages in relation to the predominant geological and tectonic conditions. In the second place, its purpose was to show the different water storages in the rock mass, their mutual relationships and their communication with the sea water reservoir with regard to the water-bearing capacity.

THE GEOLOGICAL AND GEOPHYSICAL EXPLORATION AND WORKING METHODS

THE GEOLOGICAL AND GEOPHYSICAL EXPLORATION

The geological and geophysical exploration was started in 1971 and was completed in 1973 (Larsson 1973, Moberg 1974). It included the geological mapping of exposed rocks, seismic investigations and a study of cores taken from bore-holes. A number of seismic profiles were made along the tunnel and, on the basis of these investigations, nine diamond-drilled bore-holes were placed in zones of low seismic velocity. The cores were investigated with respect to the petrography and the joint frequency. In seven of these bore-holes, a systematic test of water loss was made (Moberg 1974).

WORKING METHODS

The excavation of the tunnel has been continuously followed by an engineering and geological survey, for the purpose of obtaining information about the geological and tectonic conditions in the rock mass (Carlsson and Olsson 1976a). This survey was made in order to form a basis of judgement regarding any necessary final tunnel supports and provide further information about the rock mass for the planning of the third and fourth power-units at Forsmark. The geological mapping included investigations of the structural geology and other elements of importance for the tunnelling and the rock stability. The mapping was supplemented with rock-stress measurements along the tunnel line, in order to obtain information about the initial state of stress of the rock mass and variations of magnitude and direction between the different rocks (Hiltscher 1976). The method of measuring used is described in Hiltscher and Strindell (1976).

In order to simplify the work and for rock-mechanical and tectonic reasons, the Forsmark tunnel was divided into ten separate zones, according to the differences in these properties. The orientation of the joints within the zones was determined on the basis of the geological map drawn. It has been described for each of the rock-mechanical zones by projecting the perpendicular of the joint plane onto the lower hemisphere.

The joint plane is imagined to be placed in such a way as to cause the centre of the sphere to be located in it. The geometrical orientation of the joint is visualized by projecting the point of intersection between the perpendicular to the joint plane through the centre of the sphere and the lower hemisphere. The projection of the lower hemisphere with the point of intersection is then rectified.

Particularly interesting parts of the tunnel have been photographed, partly in stereo, for documentary purposes and also for the purpose of improving the methods of geological mapping of tunnels. Material from the clay-filled joints in the tunnel has been analysed by X-ray diffraction, in order to determine the mineral composition with respect to the possible swelling tendency of the clay minerals.

Throughout the geological mapping, a special study was made of the occurrence and the volume of the individual water leakages. In this respect, the individual leakages were connected with special joints or joint sets. The volume of the individual leakages was estimated on a three-degree scale. The total leakage into the tunnel is known and the estimated leakages have been added for the whole tunnel and adapted to the real, measured volume. To quantify the water inflow and to obtain information about the quantitative distribution along the tunnel, the estimated observations have been added for every ten metres of the tunnel. The variations of the water inflow between the zones conditioned by the rock mechanisms have been estimated by calculating a value of the leak intensity for each zone, i.e. a mean value of the water inflow into the zone per metre of tunnel.

On the basis of the systematic tests of water loss, the hydraulic conductivity of the jointed rock mass has been determined by a method described by Carlsson and Olsson (1976 b), among others. This method of measuring the tightness of a rock mass has been used as a standard method by the Swedish State Power Board. The values of the hydraulic conductivity and the seismic velocity have been used to calculate the total theoretical leakage into the tunnel.

GEOLOGY, TECTONIC FEATURES AND TUNNEL SUPPORTS

The hydraulic conditions that are of importance as regards the occurrence and movement of the water in a crystalline rock aquifer are to a very large extent dependent on the system of joints.

The tectonically conditioned zones of weakness in the rock mass determine both the infiltration of the sea water into the rock aquifer and the communication between areas of different water storages. The tectonic features of the joints are greatly dependent on the geological conditions and on the behaviour of the integral rocks in response to tectonic influence.

For rock-mechanical and technical reasons, the Forsmark tunnel has been divided into ten separate zones, designated A–K, with different properties. The characteristic properties of each individual zone are shown in Table 1 and the situations of the zones are shown in the tunnel section (Fig. 3).

TABLE 1. Characteristic parameters of the rock-mechanical zones.

Zone	Main Petrology — Structure of the rock mass	Joint sets	Estimated Rock Quality Designation	Maximum compressive stresses in the horizontal plane. Magnitude and direction	Leak intensity l/min m
A	Gneiss granite — Massive	A. N80°W; 80°S B. Horizontal	75		0.5
B	Gneiss granite — Slaty	A. E—W; 30°S B. Horizontal	45		3.2
C	Gneiss granite — Massive	A. N80°W; 80°S B. E—W; 10°S	100	15 MPa. N 24°W	1.9
D	Gneiss granite — Blocky	A. N80°W; 70°S B. N80°E; 50°W C. Horizontal	25		8.3
E	Gneiss granite — Massive	A. N80°W; 70°S B. Horizontal	80	13 MPa. N 60°W	0.4
F	Gneiss granite — Massive	A. N70°W; 80°S B. N80°W; 40°S C. Brecciated	80	14 MPa. N 45°W	0.5
G	Breccia	A. Brecciated	30		3.9
H	Paragneiss — Slaty	A. E—W; 70°S	95	9 MPa. N 24°W	1.0
I	Paragneiss — Blocky	A. E—W; 60°S B. N20°E; 80°N	30		3.5
K	Paragneiss — Slaty	A. N45°W; 70°S	100		0.4

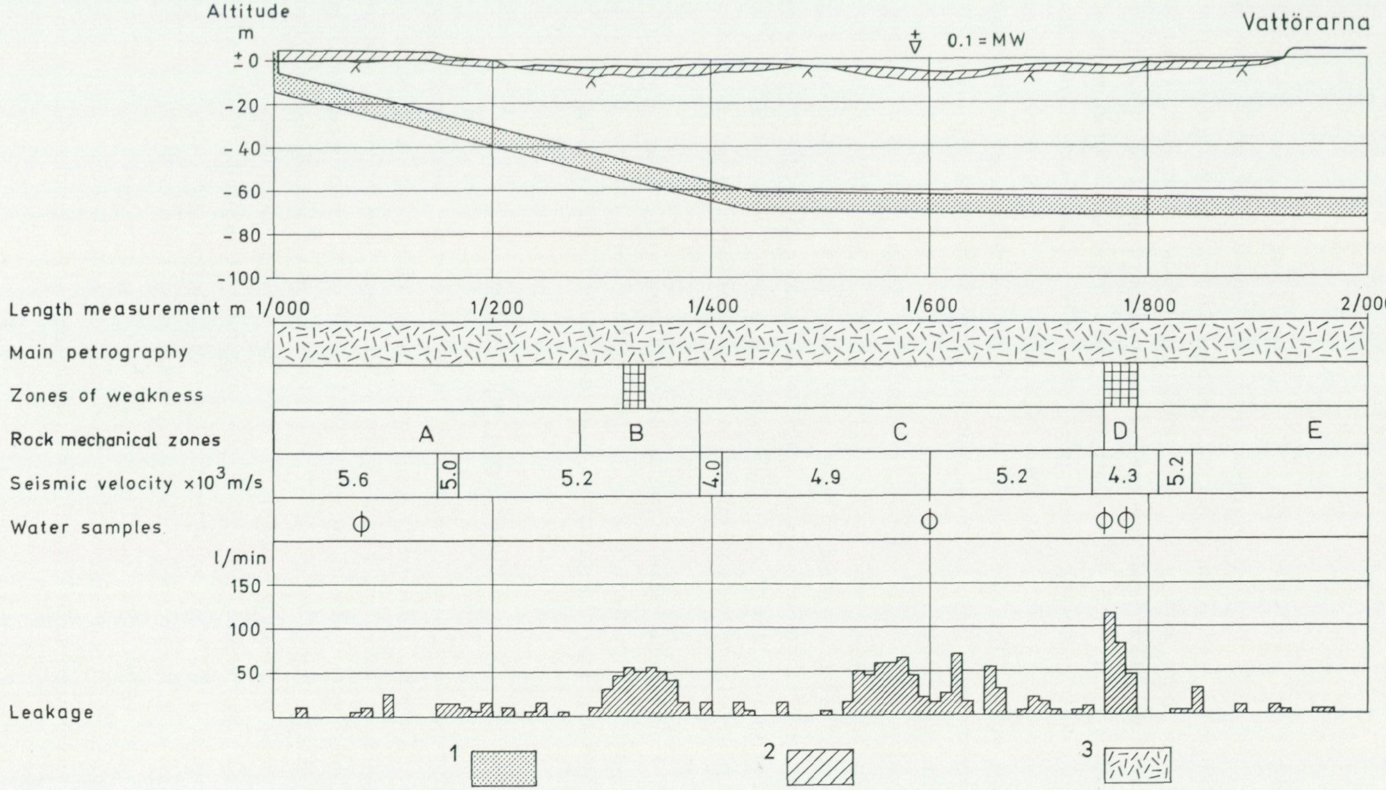

Fig. 3a. Longitudinal section through the tunnel. 1. Tunnel. 2. Soil cover. 3. Gneiss granite. 4. Brecciated gneiss. 5. Paragneiss.
Längdsektion genom tunneln. 1. Tunnel. 2. Jordtäcke. 3. Gnejsgranit. 4. Breccierad gnejsgranit. 5. Sedimentgnejs.

GEOLOGY

Schistose, old Svecofennian, intrusive rocks of tonalitic composition so-called gneiss granites, as well as mica gneisses and mica schists, here termed paragneisses, make up the main part of the Forsmark tunnel rocks. The rock traditionally called gneiss granite is from the engineering-geological point of view an orthogneiss with a rather well defined schistosity and anisotropy. Some remnants of leptite, acid-to-intermediate, fine-grained gneisses of volcanic origin, may also be found in the gneiss granite. Late dikes of amphibolitic composition in the gneiss granite, as well as dikes and/or basic layers in the paragneiss, are fairly frequent. Late Svecofennian dikes and small massifs of pegmatite make up about 10 per cent of the rock.

Due to late tectonic movements, mylonitic rocks and breccias have been developed across a 200-m-wide section of the tunnel in the gneiss granite. An example of the brecciated gneiss granite is shown in Fig. 4. In this brecciated gneiss granite, there are numerous veins of quartz and calcite. Several clay-filled joints with a maximum width of about 50 cm appear within the brecciated zone (Fig. 5). The material has been identified by X-ray diffraction as being chiefly illite and quartz.

Several calcite veins, partly forming druse cavities with crystallizations of calcite, aragonite and pyrite, are to be found. In these druse cavities, mineral pitch is very common. The rock distribution in the tunnel is shown in Fig. 6.

TECTONIC FEATURES

The tunnel intersects at a comparatively favourable angle four distinct zones of weakness (zones B, D, G and I, according to the rock-mechanical classification). These zones are shown in Fig. 3. Their widths vary between 30 m and about 200 m. The direction of both zones G and I is N 60° W, the direction of zone D is N 80° W and that of zone B E–W. All these four zones, like most of the tunnel, show evidence of shear movements, indicated by vertical slickensides.

According to Larsson (1973), the post-orogenic tectonization of the rock took place during at least six separate phases, with intermediate calcite and quartz dissemination of the crushed rock. It is possible to distinguish this course of geological events within zone G, while zone D shows just one phase of tectonization. The frequency of open joints within the brecciated zone shows a considerable increase between sections 2/450 and 2/500, while the joints are tight in the remaining part of the zone.

The joint patterns of the two predominant rocks differ from each other in that

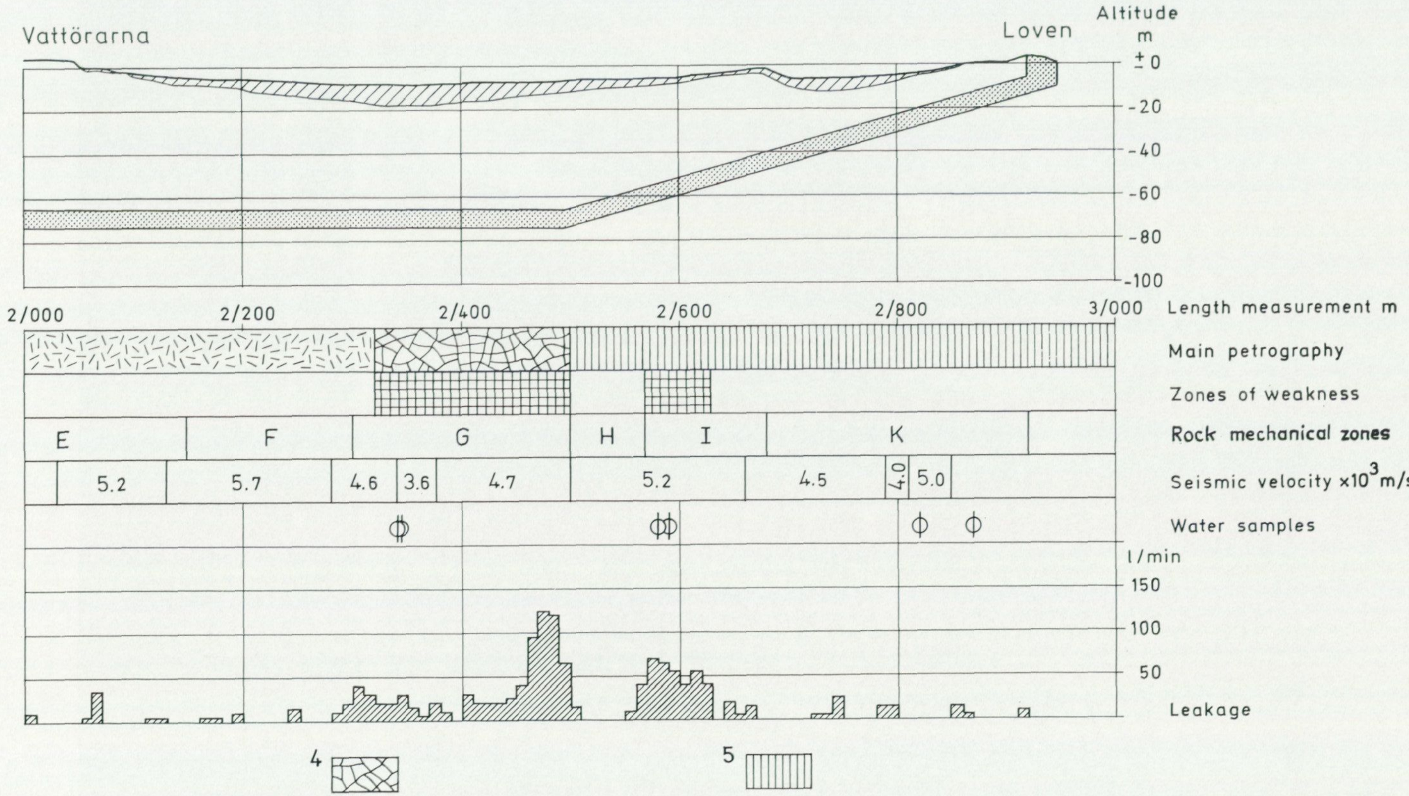

Fig. 3b. Longitudinal section through the tunnel. 1. Tunnel. 2. Soil cover. 3. Gneiss granite. 4. Brecciated gneiss. 5. Paragneiss. (See also Fig. 3a.)
Längdsektion genom tunneln. 1. Tunnel. 2. Jordtäcke. 3. Gnejsgranit. 4. Breccierad gnejsgranit. 5. Sedimentgnejs. (Se även Fig. 3a.)

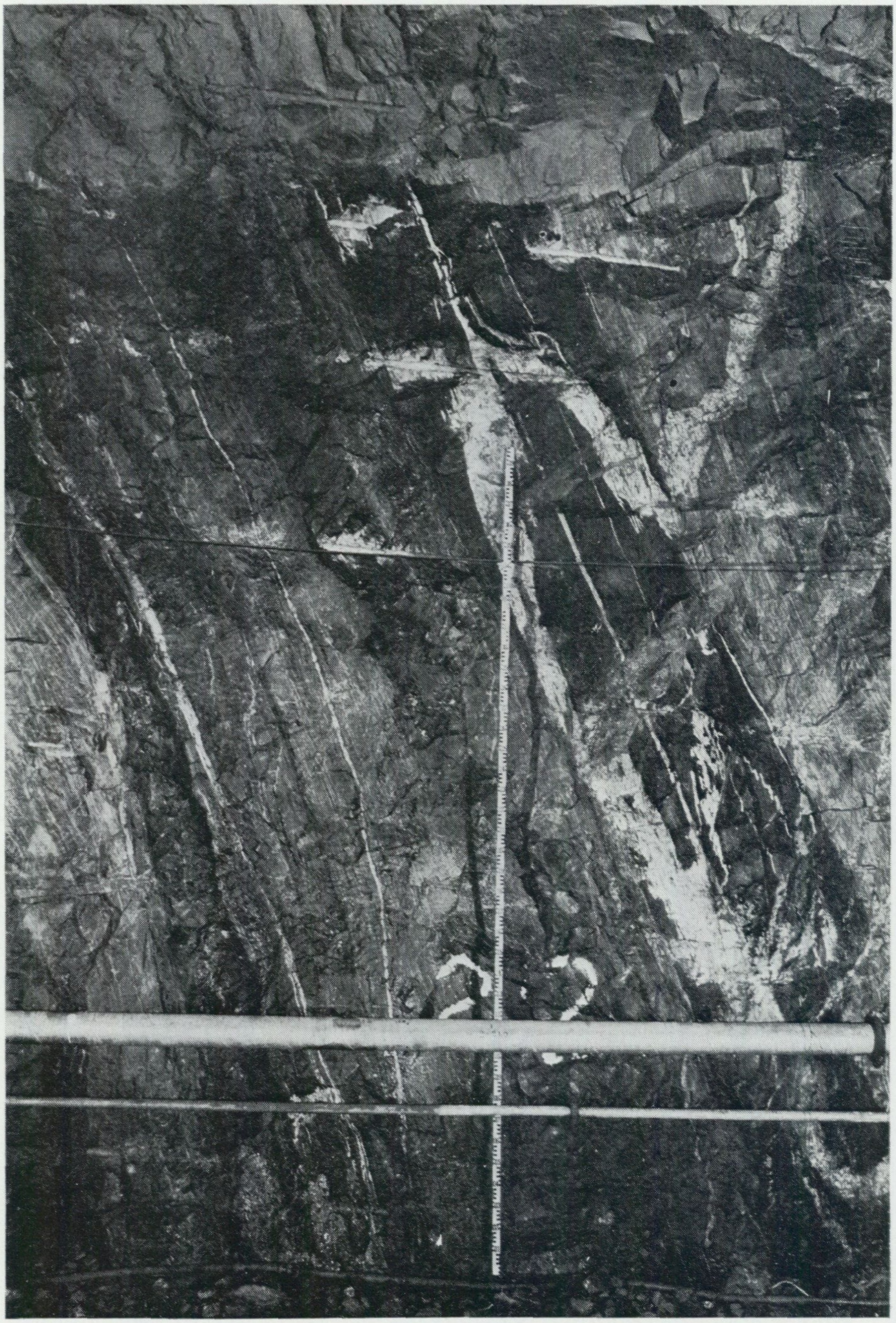

Fig. 4. Brecciated gneiss granite with numerous veins of quartz and calcite. (Photograph by G. Hansson.)
Breccierad gnejsgranit med talrika genomådringar av kvarts och kalcit.

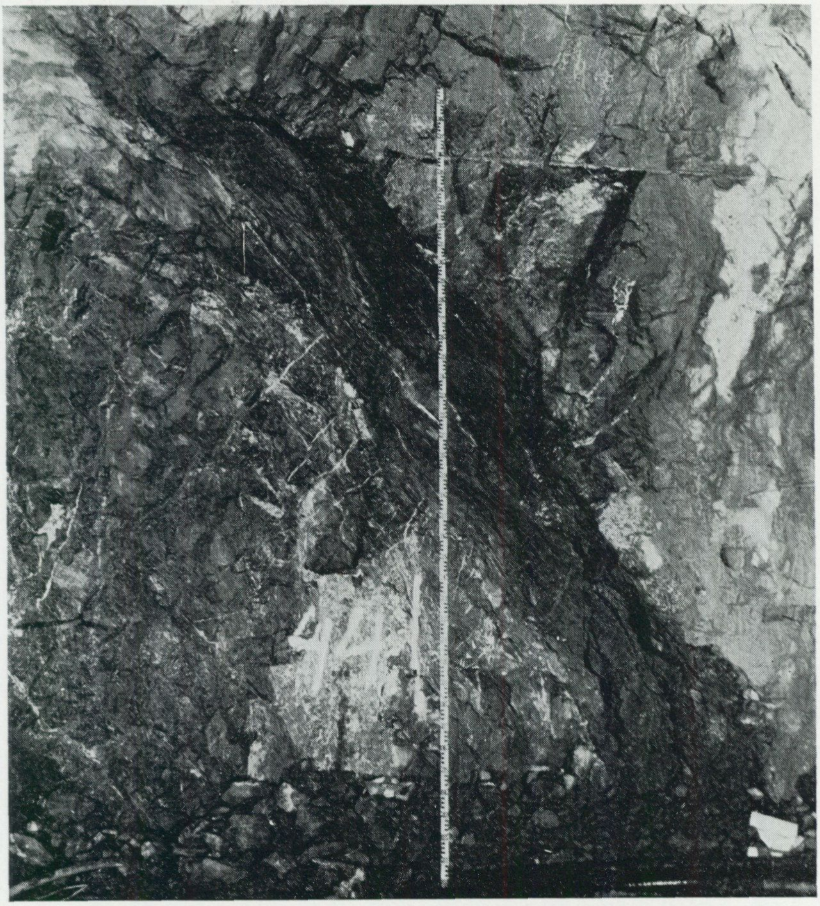

Fig. 5. Clay-filled joint in brecciated gneiss granite. (Photograph by G. Hansson.)
Lerfylld spricka i gnejsgranit.

the joint planes of the paragneiss in general correspond to the schistosity of the rock, while the gneiss granite shows a blocky structure, which is more independent of the rock structure. The paragneiss has a chiefly slaty structure, with steep joints split into smaller blocks. The fundamental difference between the structures of the two predominant rocks is shown in Figs. 7 and 8. The most frequent direction of the strike in the gneiss granite is N 60° W, while the direction that predominates in the paragneiss is N 45° W. The horizontal joint planes strike chiefly E–W. The strikes and the dips of the joints within the rock-mechanical zones will be found illustrated diagrammatically in Fig. 9 A–K.

The tectonic deformation line which the tunnel crosses may be located by interpreting aerial photographs taken from the Landsat satellites (Ehrenborg and Stephansson 1976). Interpretation of the distinct lineament structure shows that the Forsmark nuclear-power plant is situated between two zones of the first order.

ROCK-STRESS MEASUREMENTS

The values of the rock-stress measurements made by Hiltscher (1976) are shown in Fig. 10. The highest values of the compressive stresses are to be found in the gneiss granite, i.e. to the south of the brecciated zone. The direction of these stresses shows a rather good correspondence to the predominant direction of the joints.

The direction of the highest values of the stresses measured in the gneiss granite varies from N 24° W to N 60° W and the direction of the one measurement in the paragneiss is N 24° W. The direction of the lowest value of the rock-stress is N 30° E. The regional pattern of the stress distribution in the rock indicates that the highest compressive stresses are in the direction of N 45° W, which is a mean value of all the measurements. This direction is almost parallel to the gneissic structure and diverges about 35° from the main joint direction.

TUNNEL SUPPORTS

In connection with the tunnelling operations, the initial supports consisted of unreinforced and reinforced shotcrete in the top heading. These supports were supplemented with selective and methodical bolting. During the top-heading ope-

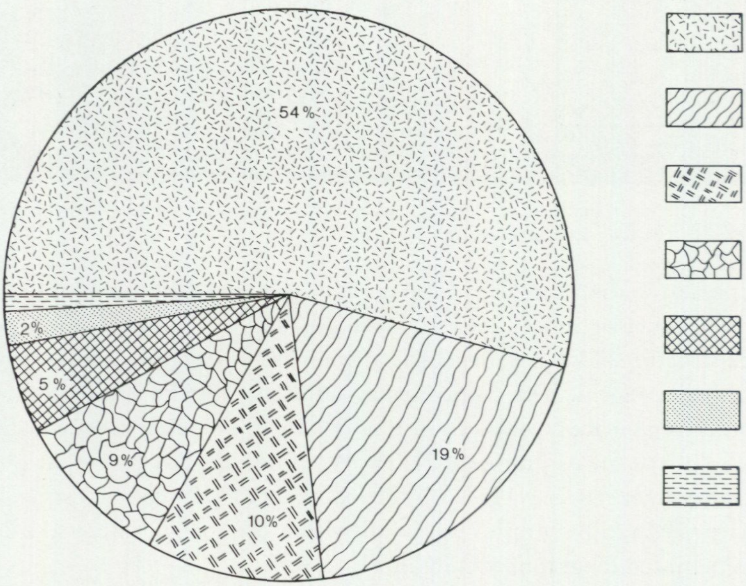

Fig. 6. The distribution of the different rock types in the tunnel. 1. Gneiss granite. 2. Paragneiss. 3. Pegmatite. 4. Brecciated gneiss granite. 5. Greenstone. 6. Leptite. 7. Mica schist.

Kvantitativ fördelning av bergarterna i tunneln. 1. Gnejsgranit. 2. Sedimentgnejs. 3. Pegmatit. 4. Breccierad gnejsgranit. 5. Grönsten. 6. Leptit. 7. Glimmerskiffer.

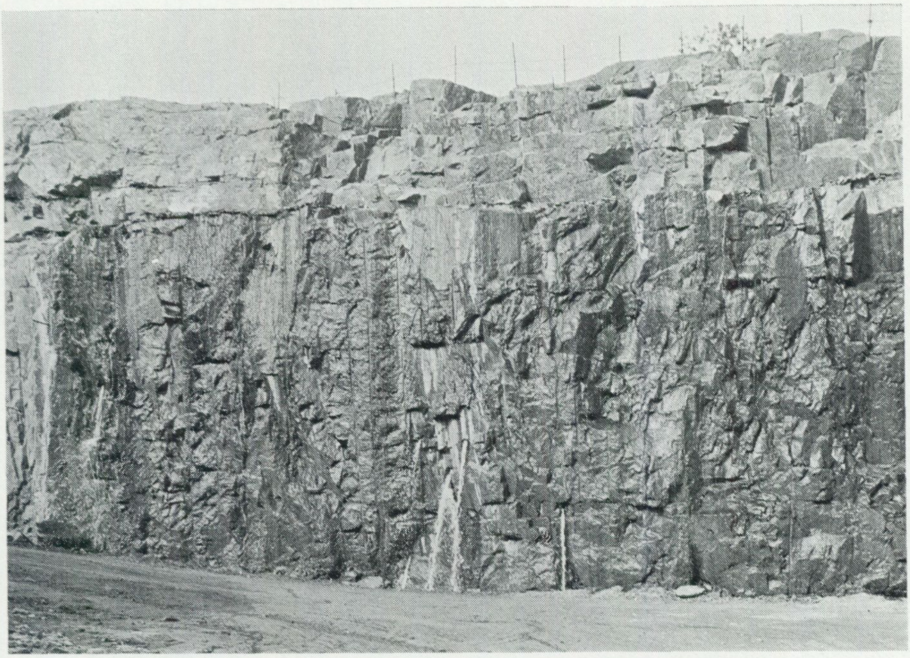

Fig. 7. The structure of the gneiss granite with water-bearing joint system formed by horizontal and vertical joint sets. (Photograph by G. Hansson.)
Gnejsgranit med horisontella och vertikala vattenförande sprickor.

Fig. 8. The structure of the paragneiss with water-bearing fissures parallel to the schistosity of the rock. (Photograph by G. Hansson.)
Sedimentgnejs med vattenförande sprickor parallella med bergartens skiffrighet.

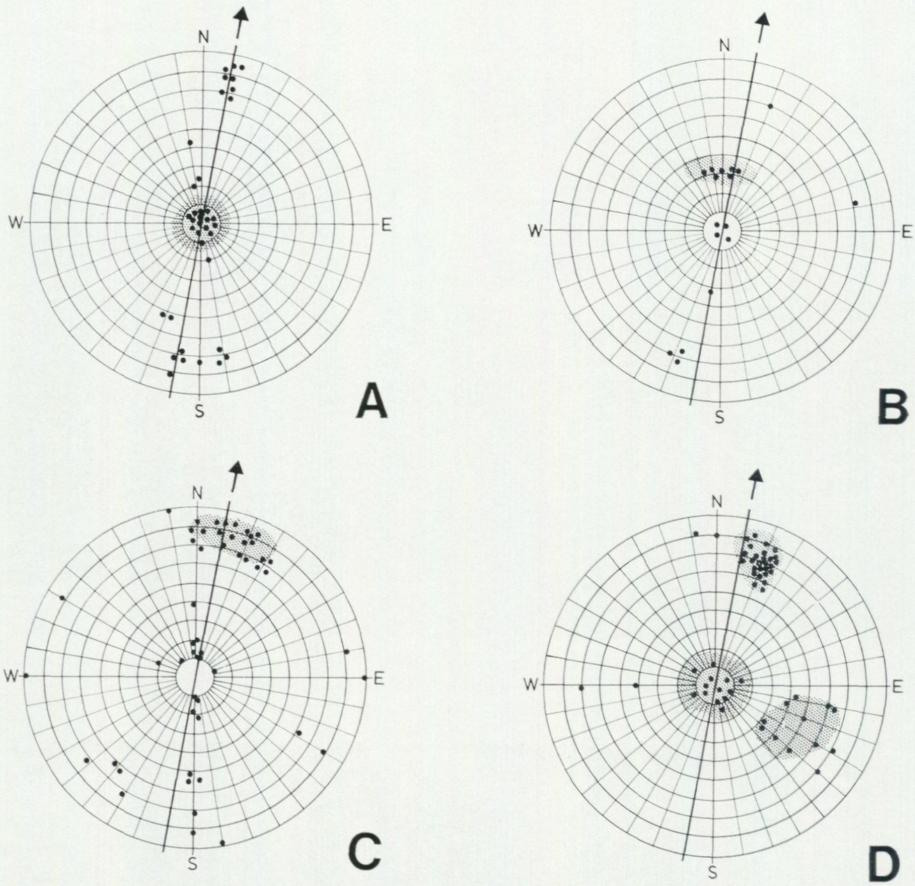

Fig. 9. Sphere projections, showing the orientation of the joint planes within the rock-mechanically conditioned zones A—K. The water-bearing joint sets are marked by a special tone. The direction of the tunnel (N10°E) is marked in each diagram.
Semisfäriska diagram som visar de, inom var och en av de bergmekaniskt betingade zonerna A—K, förekommande sprickorna. De vattenförande sprickgrupperna är markerade med raster. Tunnelriktningen (N10°Ö) är markerad i varje diagram.

rations, pre-grouting with about 115 tons of cement was carried out. The locations and the quantities of pre-grouting are shown in Fig. 11. In all, 30 arches of reinforced shotcrete were placed in the top heading.

WATER LEAKAGE

During the geological mapping of the Forsmark tunnel, special attention was given to making careful observations and recordings of the occurrence and volume

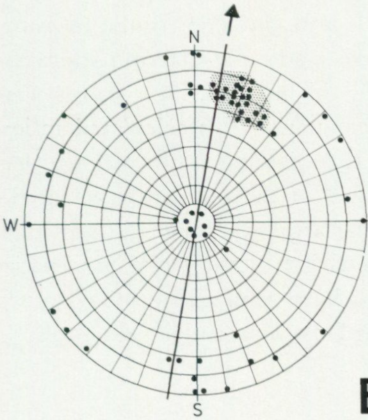

E

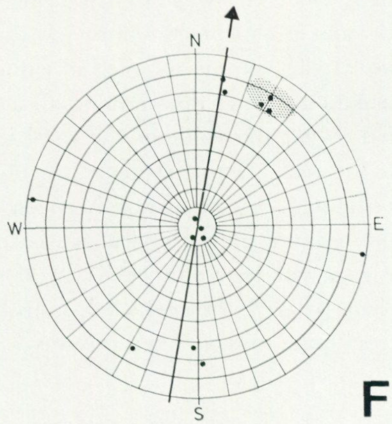

F

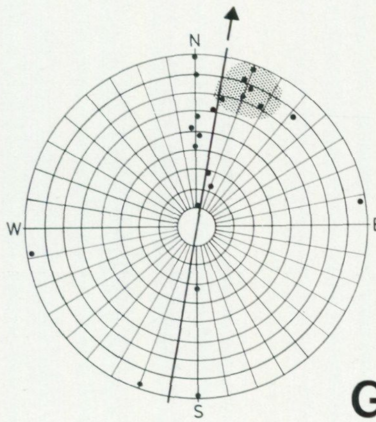

G

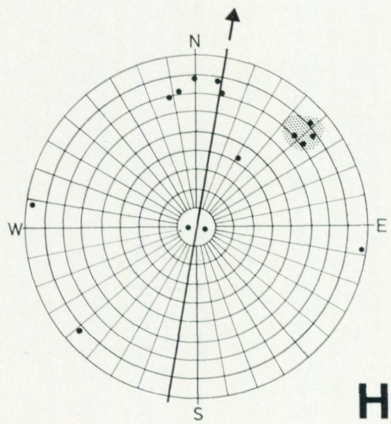

H

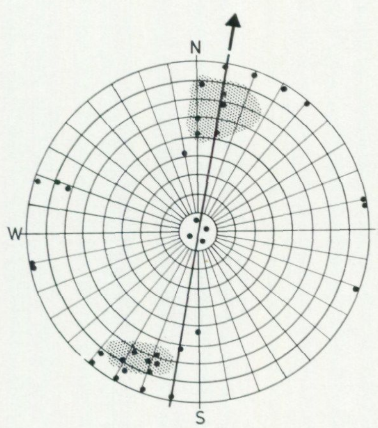

I

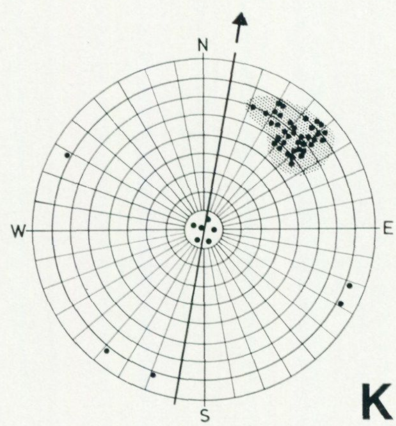

K

of each water inflow. For each inflow, the volume was determined on a three-degree scale, in which the relative ratios were 1 : 3 : 5. Because no regular measurements of the volumes of the individual leaks were made, the determinations are approximate. After determining all the inflows by this method, the volumes were added to get the value of the total inflow. By comparing this calculated inflow with the real, measured one, the volume of each individual water leakage may be estimated. A comparison between different parts of the tunnel can hardly be made, because the water leakage is represented by a great number of individual inflows of varying volumes. To make such a comparison possible and to visualize the leak pattern, the corrected, individual inflows have been added for every ten metres of the tunnel. Then the water leakage has been represented graphically in

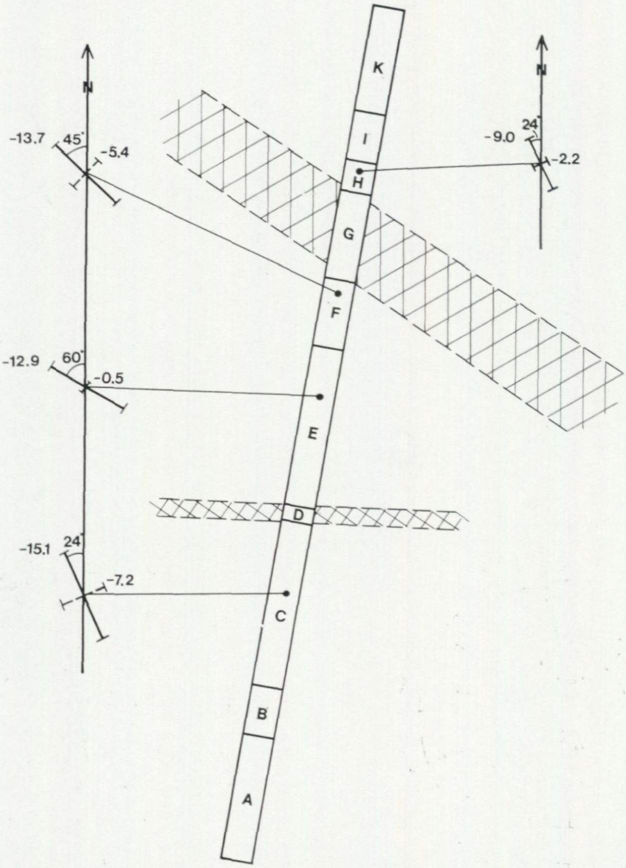

Fig. 10. Rock-stress measurements. The figure shows the direction of the stresses and the magnitude in MPa. The zones of weakness, D and G, are marked with their probable directions (after Hiltscher 1976).
Bergspänningsmätningar. Figuren visar riktning och storlek i MPa på de utförda mätningarna. Svaghetszonerna D och G är inlagda med deras sannolika riktningar.

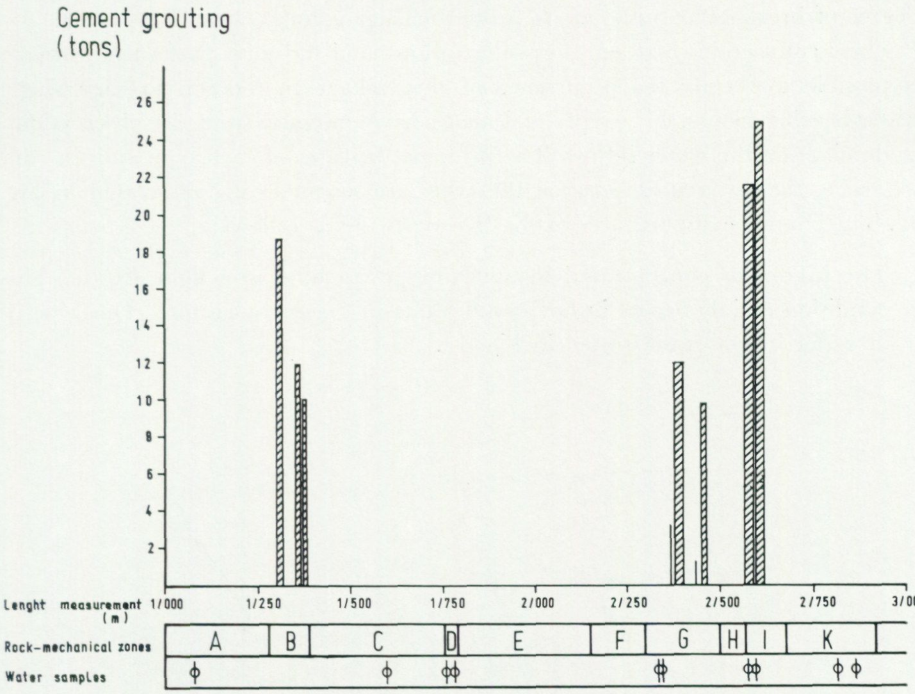

Fig. 11. Cement-grouting in the Forsmark tunnel. The sites of the grouting and the quantities of cement used are shown in the diagram.
Cementinjekterade tunnelpartier och den för varje injekteringstillfälle åtgångna cementmängden.

Fig. 3. From the individual inflows, the leak intensity, i.e. the average inflow in litres per minute and metre of the tunnel (l/min m), has been calculated for the ten zones A–K in Fig. 3. The leak intensity varies from 0.4 l/min m in the zones which have the smallest inflows up to 8.3 l/min m in the most productive zone. These leak intensities may be compared with the intensity of 1.6 l/min m applicable to the tunnel as a whole. This leak intensity is based upon the total measured inflow of 3000 l/min. Hence, the volume of the water inflow varies greatly along the tunnel site and this variation is due to the different geological and tectonic properties of the investigated rock mass.

WATER LEAKAGE AND WATER-BEARING FISSURES (FISSURE ZONES)

The general occurrence of the individual water inflows seems to follow certain patterns in relation to the different joint sets and joint systems of the rock mass at the tunnel site. Also, the varying leakage volumes and the degree of tectonic disintegration are in well-defined agreement with each other. Normally, a high degree of breakage corresponds to a high leakage volume.

These connections between the water inflows and the joint pattern have made it possible to classify the occurrence of the leakage in relation to each single water-bearing fissure. Five types of leakage have emerged from the observations, as dominating the water inflow. The principal features of each type and, in consequence, the differences between the types are schematically illustrated in Fig. 12. The characteristic features of the five types are as follows:

1. The leaking is concentrated in apertures in an otherwise tight fissure. This condition mainly occurs in horizontal joints in the gneiss granite. This type of of water inflow is illustrated in Fig. 13.

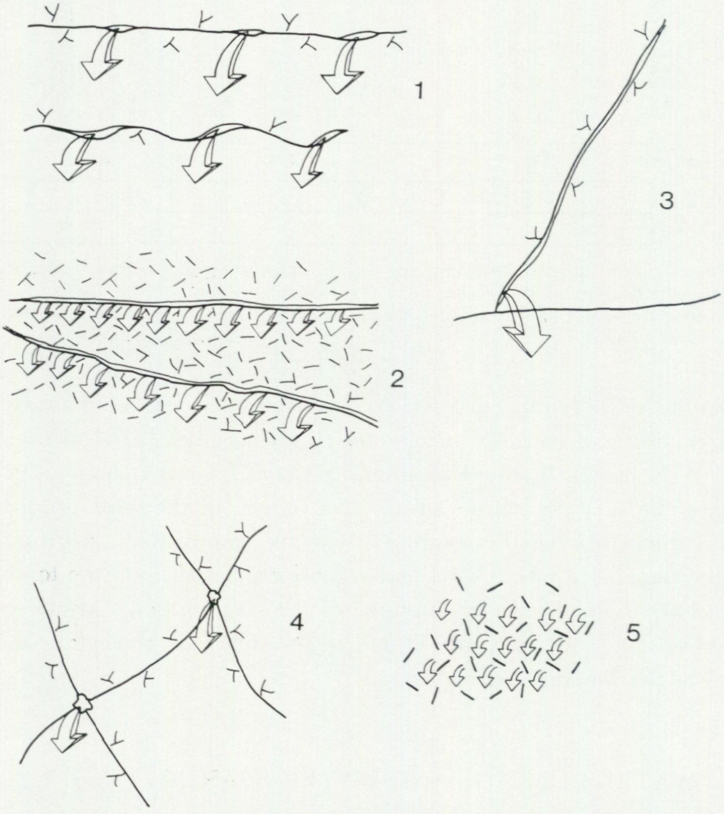

Fig. 12. Schematic illustration of the different appearances of the water inflows. 1. Aperture in a horizontal fissure. 2. The inflow along a horizontal or medium-steep fissure with no apertures but is often distinct. 3. Inflow at the lower limit of a steep fissure. 4. Inflow at the crossings of fissures. 5. Diffuse water inflow.
Schematisk illustration av de förekommande läckagetyperna. 1. Flack spricka med hål. 2. Flack eller medelbrant spricka utan hål. 3. Brant spricka med läckaget koncentrerat till sprickans nedre begränsning. 4. Korsande sprickor. 5. Diffust läckage.

2. The water inflow occurs along horizontal or medium-steep fissures, often as a distinct flow without noticeable apertures. This type is shown in Fig. 14.

3. The water leakage occurs in steep fissures, generally as distinct inflows at a lower boundary of the fissure or on the tunnel floor.

4. Distinct inflows at crossings between two or more fissures. Generally, no inflows or only very small ones occur along the individual joint planes outside the crossing-points.

5. The water leakage occurs as a diffuse inflow or flows out of the rock on a broad front. In general, no distinction between different inflows is noticeable and no correspondence between a certain water inflow and a certain fissure is to be found.

One of these types of leakage usually predominates in the inflow pattern in each of the ten zones. But, while it is obvious that one of the types predominates, this type is not alone responsible for the whole inflow. In most zones, all the five types of leakage may be found.

In general, the laminar flow capacity within a fissure is in direct proportion to the third power of the free opening of the fissure and to the length of the fissure (Lomize 1951, Louis 1967 and others). From this, it is obvious that the widths of the fissures are of the greatest importance for the hydraulic conductivity of a jointed rock mass. The width of the water-bearing joints is normally less than 1 mm. In the Forsmark tunnel, this circumstance is verified by the fact that the types in which the water inflow is related to apertures or local widening of the fissures normally have the largest flow volumes. Hence, the first and the fourth of the five types, which both satisfy this condition, have the largest volumes for the individual fissure. The occurrence of a leakage of type 1, apertures in horizontal fissures, is usually caused by dilatation and widenings due to movements at the joint planes. For the fourth type, the water inflow is related to the crossing-points between fissures, and the widening is due to crushing of the rock (cf. Fig. 12). Water leakage of type 4 gives rise to the highest total volume. But this condition is not dependent on the quality of the individual fissures but mainly on the fact that type 4 is very common in the four tectonic zones of weakness, where the frequency of fissures and thereby the frequency of crossing-points is high. The capacities of the individual fissures are as high in type 1 as in type 4. Normally, the inflows of these two types are persistent and no decrease or increase of the volume is to be discovered in process of time.

Generally, only small leakage volumes are due to inflows of type 3, water inflows in steep fissures. The volume of leakage of this type often decreases over time and in many fissures the inflows have stopped.

Fig. 13. Water inflow from an aperture in a horizontal fissure. Large quantities of iron and manganese sediments are to be found at the aperture. (Photograph by G. Hansson.)
Inläckning från hål i flack spricka. Stora mängder järn- och mangansediment är avlagrat i anslutning till läckagepunkten.

Types 1, 2 and 5 are responsible for a great deal of the total inflow to the tunnel. For the individual fissures in these types, the capacities vary within wide limits, from almost nothing to considerable flow volumes. Normally, the water inflows are persistent, though they have stopped in many fissures.

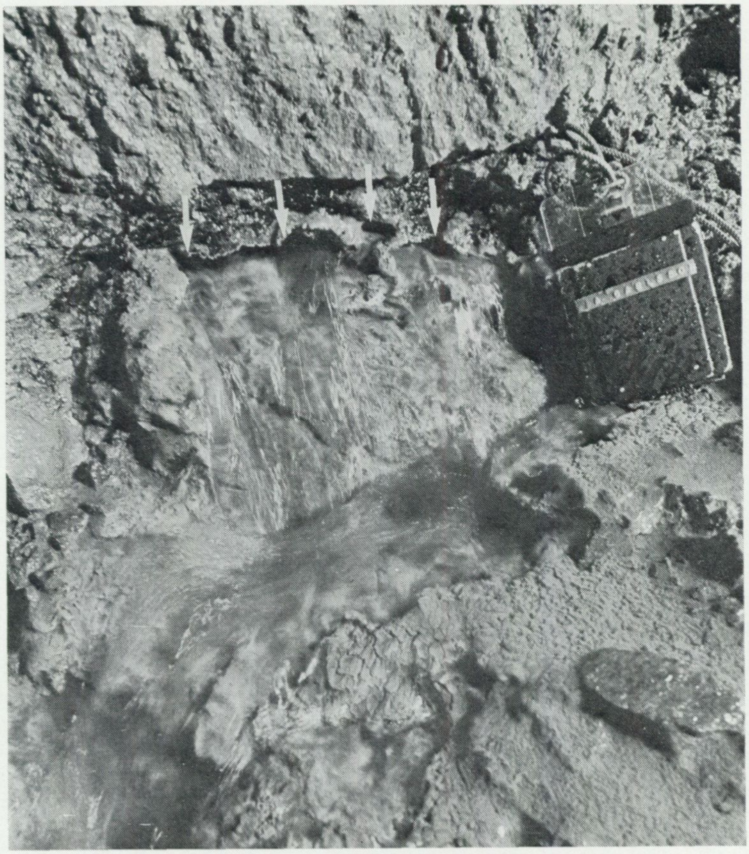

Fig. 14. Distinct inflow from a horizontal fissure with no apertures. (Photograph by G. Hansson.)
Läckage från flack spricka utan hål.

THE WATER INFLOW RELATED TO THE ROCK-MECHANICAL CLASSIFICATION

The bedrock in the tunnel is very heterogeneous, not only with respect to the degree of breaking but also to the occurrence and the volumes of the water inflows. Heavily jointed parts of the tunnel with large inflows alternate with completely tight and dry parts. Because of this heterogeneity, it has been necessary to divide the tunnel site into smaller parts, where each part may be regarded as a homogeneous unit. On a rock-mechanical basis, the tunnel was divided into ten separate zones and this division has turned out to be suitable for the water leakage as well. The occurrences of the water inflows are alike within each of the ten zones (zones A–K in Fig. 3), while the differences are great between different zones.

The strikes and the dips of the different joint sets which are important for the

TABLE 2. Characteristic features of the water leakages in the different rock-mechanical zones.

Rock-mechanical zone	Predominant group of water leakages	Water-bearing joint sets	Leak intensity l/min m	Sediment occurrence Common (C), Mediocre (M), Rare (R)
A	1, (3,4)	Horizontal	0.5	C
B	2	E—W; 30°S	3.2	R
C	3, (1,5)	N70°W; 80°S	1.9	M
D	4,5	N70°W; 70°S N20°E; 60°W	8.3	C
E	3	N70°W; 70°S	0.4	M
F	3, (1)	N60°W; 80°SW	0.5	R
G	4,5	N70°W; 80°S	3.9	M
H	3	N40°W; 80°SW	1.0	M
I	4	N80°W; 70°S N70°W; 70°N	3.5	C
K	3	N50°W; 70°SW	0.4	R

water inflow are reported for each zone in Table 2. In the same table, the predominant types of leakage and the occurrence of sediments are also reported. Fig. 9 A–K shows the geometrical orientation of the fissures in the zones. The joint sets of importance for the water inflow are marked by a special tone.

The tectonic zones of weakness, zones B, D, G and I, have the highest water inflows and, in all, about 60 per cent of the leakage comes from those zones. The total length of these zones is approximately 450 m of the total of 1921 m. Those proportions give a leak intensity of about 4 l/min m for the zones of weakness, which may be compared with the leak intensity for the rest of the tunnel of only 0.8 l/min m. The brecciated zone G is, owing to its length, the most productive of the four tectonic zones and about 25 per cent of the total inflow to the tunnel has its origin here.

Within zone G, the leakage is very unequal, so that half of the zone is dry, while the inflow is concentrated in the other half. This is evident from the flow figures given in Fig. 3. Zone D has the highest leak intensity of all the zones (8.3 l/min m). This leak intensity is about 20 times as great as that in the driest zones and more than double that in the other tectonic zones.

Zones A, E, F and K all represent parts of the tunnel with very small volumes of leaking water and large stretches of these zones are completely without inflows. Generally, the inflows show a decreasing course in those zones, except in zone A, where the inflow is persistent.

During the tunnelling, some parts of the rock mass were cement-grouted and probably this operation caused a decreased inflow, due to the original hydraulic conductivity. Fig. 11 shows the grouted parts of the tunnel and the quantities of cement used.

WATER LEAKAGE IN DIFFERENT ROCK TYPES

The occurrence of leaking water and the leak intensity shows great differences as between the two dominating rock types at the tunnel site. The leak intensity in the gneiss granite, excluding zone G, is 2.3 l/min m. The corresponding value in the paragneiss is 1.3 l/min m. In this respect, by regarding the two rock massifs as units, the difference may be fairly well defined. However, zones A and K, which are both situated near the surface in the two rocks respectively, show only a slight predominance of 0.54 l/min m in zone A to 0.42 l/min m in zone K.

Usually, the water-bearing fissures in the paragneiss are included in the schistose structure of the rock mass, while the fissures and thereby the water inflows in the gneiss granite seem to occur more independently of the rock structure. These conditions produce the significant difference in occurrence and capacity between the two main rock types. With respect to the tectogenesis which has created the water-bearing fissures, the two main rock types show different behaviours. In the gneiss granite, the jointing shows a regular pattern. The horizontal joint sets are cut off by vertical joint sets. This rectangular network of fissures forms at least one, co-operative water-bearing system. In the paragneiss, no such co-operative system is developed and the joint sets are dominated by the schistose rock structure. The structure of the two main rocks is shown in Figs. 7 and 8. In the gneiss granite, the horizontal joint set is especially well developed near the rock surface but seems to vanish at greater depth.

In an earlier investigation (Carlsson and Olsson 1976b), this fact was attributed to hydraulic causes. The hydraulic conductivity of the gneiss granite, decreases greatly as the depth increases. According to Wenner (1951), it is usual for the water-bearing systems to be better developed in granitic rocks than in gneissic ones. Normally, wells in granitic rock have the highest capacities. The opposite condition is present within the south-western Swedish gneiss region, where gneissic rocks normally have the highest capacities (Palmqvist 1974). Palmqvist assumes that the difference in capacity between different rock types is associated with different properties, due to the tectogenesis, for example, the possibilities of the development of clay-filled joints and slickensides and/or the possibilities of fracturing.

WATER STORAGES IN THE ROCK MASS

From the description of the occurrences of water in the different zones, it is obvious that the water content and the water movements within the rock mass can be assigned to several limited aquifers or even aquicludes. In relation to the occurrences and the volumes of the water inflows, it is possible to regard the ten zones as isolated aquifers with either positive or negative hydraulic boundaries at the zone borders. Generally, the boundaries correspond to an increase or a decrease of the hydraulic conductivity, but in some zones the aquifers are surrounded by impervious layers. In the latter case, no exchange between the aquifers is possible.

Usually, the hydraulic conductivity within each zone is almost constant, while it varies between different aquifers. The communication between different aquifers is poor and the communication between the rock mass and the overlying sea in some of the aquifers is also very poor.

The zones with small inflows act as isolated aquicludes, with no communication with possible infiltration sources. In zones E, F and K, the leakage volume tends to decrease with time. This behaviour of the inflow shows that the rock mass is being drained. Obviously, the infiltration to these zones is low and therefore cannot balance the drainage. The structure of the rock, with almost vertical schistosity and fissures, would be favourable for infiltration from the sea, but the soil cover on the rock surface probably has limiting effect on the infiltration ratio. According to Hagerman (1956), an infiltration of cold water may tighten the fissures, due to air clogging.

Infiltration from the surrounding aquifers is prevented by the rock structure. The strike of the schistosity planes and fissures with mineralization is almost parallel to the strike of the tectonic zones and hence the hydraulic conductivity perpendicular to the structure is probably very low. Especially in the paragneiss, fissures crossing the schistosity are rare, but also in the gneiss granite the crossing system is not so well developed in those zones.

Zones A and C represent a second type of aquifers and both these zones are situated in the gneiss granite fairly near the rock surface. In these zones, the horizontal joint set is well developed and the conditions for infiltration are favourable. As mentioned above, the water inflow is persistent and the infiltration balances the drainage.

A special type of aquifer is formed by the four tectonic zones of weakness, zones B, D, G and I. Generally, the water inflows in these zones have large volumes and are persistent. These conditions indicate that the communications with the sea are direct and of considerable width. The hydraulic conductivity must be very high to permit the large volumes. In zone G, the calcite veins and the clay alteration are of great importance, as they tighten some parts of the zone. The disseminated part of the zone has a rather low capacity in relation to the part which was affected by the latest tectonic phase.

The different water storages of the rock mass and the established hydraulic boundaries are schematically shown in Fig. 15. The tightnesses of the three different types of storages are marked by different tones. The hydraulic boundaries have also been differentiated into three groups with varying degrees of tightness. Depending on the varying hydraulic characteristics of two closely located storages, the separating boundary will have different characteristics. The boundary of the first storage may be a tight, hydraulic boundary, while the same boundary of the second storage may be untight. Depending on these conditions, the boundaries in Fig. 15 are related to the storage with the smallest water penetration. The following values of tightness have been used to describe the characteristics of the boundary:

1. The tightness of the boundary corresponds to the tightness of the storage.
2. The boundary is tighter than the storages, but there is a certain amount of water penetration.

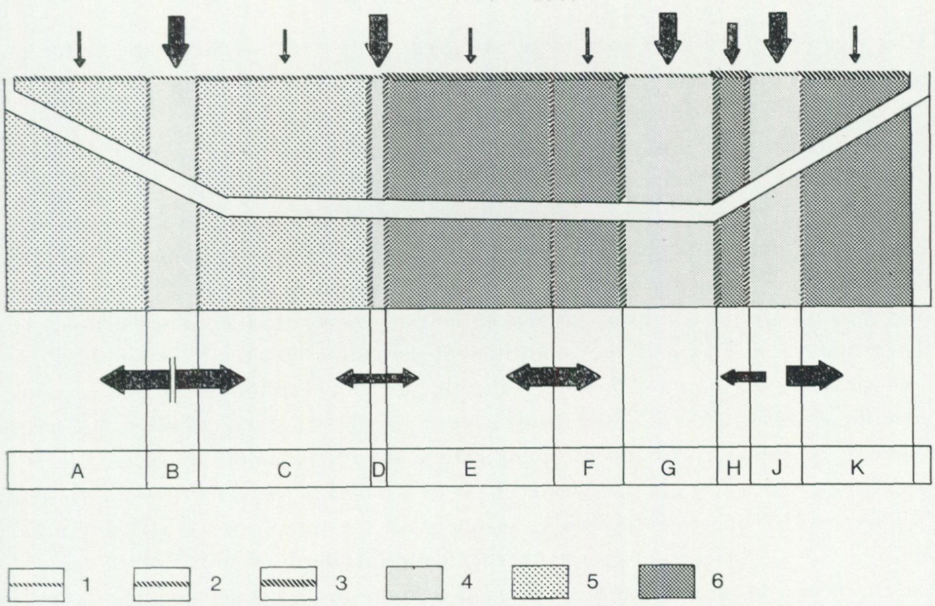

Fig. 15. An outline of the different water storages and their communications in the rock mass along the tunnel. The relative hydraulic conductivity of the rock mass and the relative tightness of the hydraulic boundaries are illustrated by different tones. 1. Untight boundary, large infiltration. 2. Tight boundary, medium infiltration. 3. Very tight boundary, little or no infiltration. 4. Rock mass with high hydraulic conductivity. 5. Rock mass with medium hydraulic conductivity. 6. Rock mass with low hydraulic conductivity.

Schematisk bild av bergmassans olika vattenmagasin och kommunikationsvägar längs tunnellinjen. Bergmassans relativa permeabilitet och de hydrauliska gränsernas relativa täthet illustreras av olika raster. 1. Otät gräns, hög infiltration. 2. Tät gräns, måttlig infiltration. 3. Mycket tät gräns, ingen eller ringa infiltration. 4. Bergmassa med hög permeabilitet. 5. Bergmassa med måttlig permeabilitet. 6. Bergmassa med låg permeabilitet.

3. The boundary is much tighter than the storage. No or very little water penetration.

The arrows in Fig. 15 denote the water penetration in proportion to the tightness of the boundary.

CHEMICAL ANALYSIS

During the geological mapping of the tunnel, ten samples of the leaking water and one sample of the sea water were collected and analysed. The sampling sites are shown in Figs. 3 and 11 and the results of the chemical analysis are summarized in Table 3.

WATER ANALYSIS

It is clear from Table 3 that there are great differences between the different samples, not only between the leaking water and the sea water but also between the different samples of leaking water.

The initial supports may have influenced the chemical composition of the water. Obviously, the cement-grouting done during the tunnelling has caused a change in the chemical composition, but other forms of support, such as shotcrete and bolting, may also have had an influence. Water samples collected near to cement-grouted areas are impaired by a remarkably high value of the total hardness in comparison with samples from other parts of the tunnel. The locations of the cement-groutings and the quantities of cement used are shown in Fig. 11. The sampling sites are also indicated in this figure. The influence of the cement-grouting can be traced not only in the greater hardness but also in other chemical elements (Table 3). The specific conductance has its maximum in samples 2/345 and 2/580, which were both collected near to grouted parts of the tunnel.

The total hardness of the leaking water in all the samples is remarkably high, and not only in the cement-grouted zones. Sample 1/780 in zone D has the highest total hardness of all the samples collected in non-grouted zones and the value is almost twice as high as that of the reference sample. It is also possible that the high total hardness is due to the high limestone content in the soils in this area (Gillberg 1967).

One of the most striking differences between the leaking water and the sea water is shown in the pH values. In spite of the high total hardness of the leaking water, the pH value is remarkably low, compared with that of the sea water.

The iron content is much higher in the ten water samples from the tunnel than in the reference sample. The highest content is present in samples 2/340 and 2/345, and in these two samples the iron content is about 200 times higher than in the

TABLE 3. Chemical analyses of water samples from the discharge tunnel.

Sample section			1/080	1/600	1/760	1/780	2/340	2/345	2/580	2/590	2/820	2/870	Sea water
Date collected			23/6/76	16/1/76	23/6/76	16/1/76	23/6/76	16/1/76	16/1/76	23/6/76	23/6/76	16/1/76	23/6/76
Specific conductance, μ S			7900	8600	8800	8650	9500	12000	11000	8400	8400	8650	8.00
pH			7.55	7.1	7.3	7.1	7.25	7.05	7.15	7.6	7.35	8.05	8200
Permanganate	($KMnO_4$),	mg/l	21	23	18	19	18	24	26	19	19	25	17
Hardness	(Ca),	mg/l	480	550	688	750	672	970	1200	527	575	450	427
Iron	(Fe),	mg/l	1.45	3.7	3.0	3.9	6.8	7.8	4.7	1.4	3.95	0.08	0.04
Manganese	(Mn),	mg/l	0.43	0.65	0.76	0.75	0.98	1.48	1.55	0.56	0.60	0.02	0.02
Bicarbonate	(HCO_3),	mg/l	131	129	113	120	127	144	110	102	121	93	73
Chloride	(Cl),	mg/l	2950	3290	3200	3390	3450	4690	3620	3050	3100	3350	3050
Sulphate	(SO_4),	mg/l	270	280	276	260	276	220	300	290	264	300	276
Ammonium	(NH_4),	mg/l	0.84	2.6	1.6	1.8	2.5	3.6	3.1	1.7	0.54	0.11	0.09
Nitrite	(NO_2),	mg/l	<0.01	0.01	<0.01	0.01	0.02	0.04	0.02	0.01	0.14	0.01	<0.01
Nitrate	(NO_3),	mg/l	0.06	0.09	0.08	0.14	0.10	0.22	0.30	0.09	0.19	0.43	0.10
Fluoride	(F),	mg/l	0.9		1.3		1.4			0.9	1.1		0.3

sea water and about twice as high as in the other samples from the tunnel. These samples were both collected in the brecciated zone G and hence it follows that the conditions for the release of minerals, for instance pyrite, may be more favourable, because of the high degree of crushing. It is also probable that the rock-bolting in the zone may have had an influence on the iron content. In general, the same conditions and variation pattern are present for the manganese content as for the iron content.

The chloride content of sample 2/345 is about 50 per cent higher than that of the reference sample. In all the other samples of the leaking water, the chloride content is in much better agreement with that of the sea water, but, in general, it is somewhat higher in the leaking water. This condition is probably due to a salinity variance in the sea water. The water which infiltrates into the rock may have a somewhat higher chloride content than the reference sample.

The content of ammonium in the leaking water is much higher, compared with that in the sea water. This is probably due to an exchange with the sediments in the sea during the infiltration. A comparison between the different nitrogen combinations shows a greater degree of oxidization in the sea water. Such variations are generally due to variations in the conversion velocity. It is also possible that the variations of the contents of nitrite and nitrate have been influenced by the nitrous fumes during the tunnelling. As regards fluoride, the highest contents are to be found within the zones of weakness, especially in zone D and G. Normally, the highest contents of fluoride will be found in aquifers where the conversion velocity is low. This fact has been pointed out by, among others, Möller, Engqvist and Müllern (1976), who compared the fluoride content and the age of the water. From this comparison, it was concluded that the fluoride content increases with increasing age. Here, in the Forsmark tunnel, the highest fluoride contents are present in zones D and G, which are both zones of high water inflows and thereby of fast conversion velocities. Hence, the high fluoride contents in these zones may be due to an exchange of ions within the clay-filled joints.

No noteworthy differences are to be found between the leaking water and the sea water, as regards the contents of other chemical elements analysed. Sample 2/870, from a site near the rock surface, shows the best agreement with the reference sample.

SEDIMENT SAMPLES

Two samples of sediments deposited by the leaking water have been analysed. The result is shown in Table 4.

The iron content is very high in both samples, but sample 1/760 has a slight predominance of 15 per cent. On the other hand, the manganese content is nine times higher in sample 1/150. In both samples, the contents of organic materials

TABLE 4. Chemical composition of sediments deposited by the leaking water.

Sampling section			1/150	1/760
Iron	(Fe_2O_3),	%	57.8	72.9
Manganese	(MnO_2),	%	4.5	0.5
Calcium	($CaCO_3$),	%	8.3	9.0
Magnesium	(MgO),	%	1.8	<0.1
Sodium	(Na_2O),	%	3.5	1.0
Potassium	(K_2O),	%	0.1	<0.1
Organic material + bound water		%	24.0	16.5

and bound water are about 20 per cent. The sediments mainly occur in zones A, D and I.

SEISMIC INVESTIGATIONS AND TESTS OF WATER LOSS

SEISMIC INVESTIGATIONS

During the geological and geophysical site exploration (Larsson 1973, Moberg 1974), a number of seismic profiles were made along the tunnel. On the basis of the data from the first profile, a number of additional profiles were made in order to obtain further information about the strikes of the recorded zones of low seismic velocity. The recorded velocities of the first seismic profile will be found in Fig. 3.

SEISMIC VELOCITIES AND WATER INFLOWS

Here, an attempt is made to correlate the seismic velocity and the hydraulic conductivity of the rock mass. The seismic velocity and the leak intensity along the tunnel line, based on the observations made during the geological mapping of the tunnel, have been presented in Fig. 16. The parameters within the zones of weakness are proportionately in agreement with each other. The zones of high volumes of inflow and the corresponding zones of low seismic velocity are especially marked in Fig. 16. The possible correlation in zones B and I is asymmetrical along the tunnel line. However, this condition is, at least in zone B, in accordance with the tectonic view of these zones.

In Fig. 16, some of the zones of low seismic velocity do not correspond to any increased leakage into the tunnel. For example, this condition holds for the zones at sections 2/080 (3000 m/s) and 2/200 (4000 m/s). No geological indications could be discovered during the geological mapping of the tunnel which could explain these low seismic velocities.

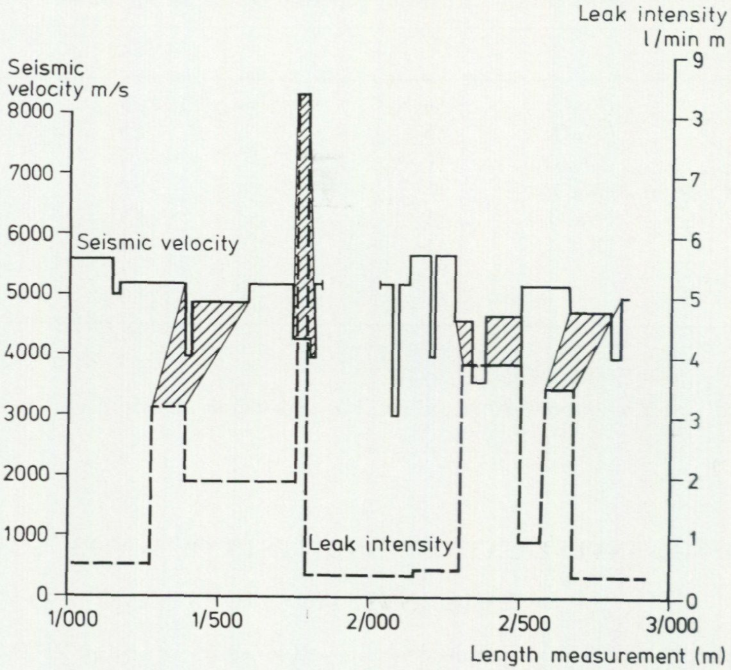

Fig. 16. Correlation between seismic velocity and leak intensity. The leak intensity is given in litres per minute and metre of tunnel. In the diagram, the shaded areas show the possible positive correlations between low seismic velocity and high leak intensity.
Korrelation mellan seismisk gånghastighet och läckageintensitet. Läckageintensiteten anges i liter per minut och meter tunnel. De streckade områdena visar de tänkbara positiva korrelationerna mellan låg seismisk hastighet och hög läckageintensitet.

It has already been mentioned that clay-filled joints have been observed in zones D and G. It is probable that these fillings have a sealing effect on the rock mass and thereby reduce the total water leakage into the tunnel.

TESTS OF WATER LOSS

Systematic tests of water loss have been made in seven of the nine bore-holes along the tunnel line (Moberg 1974). On the basis of the results of these tests, the hydraulic conductivity of the rock mass has been determined by a method described by Carlsson and Olsson (1976b). This method is used as a standard method by the Swedish State Power Board for determining the hydraulic properties of a rock mass.

In general, double packers were used, but single packers were also used in some of the measurements. A distance of two or three metres between the packers was used in these measurements. The procedure was as follows. Water under a certain pressure was forced into the rock mass between the two packers and the water loss was measured for a specific time. The hydraulic pressure was gradually increased up to a maximum of about 785 kPa (8 kp/cm^2), after which the pressure was gradually relieved. According to Banks (1972), the value of the hydraulic conductivity may be calculated from equation (1):

$$k_n = \frac{Q}{LHt} \quad C \qquad (1)$$

where k_n = hydraulic conductivity of the rock mass in test interval n
Q = water loss
L = length of the test interval
H = hydraulic pressure
C = constant
t = duration of measurement

The equation (1) is valid in the case of laminar-flow conditions, but as a fairly good approximation it may also be used for turbulent-flow conditions.

The constant C has been determined by Moye (1967) as:

$$C = \frac{(1 + \ln (L/d))}{2\pi} \qquad (2)$$

where d = the diameter of the test interval.

The value of the constant of the hydraulic conductivity was calculated for each measuring range, after which a weighted arithmetical mean was calculated for each borehole, according to the equation:

$$k = \frac{1}{\sum_{n=1}^{m} L_n} \cdot \sum_{n=1}^{m} L_n \, k_n \qquad (3)$$

where k = the hydraulic conductivity of the rock mass
L_n = the length of the test interval n
k_n = the hydraulic conductivity of the test interval n

The results of the determinations of the hydraulic conductivity will be found in Table 5, in which a calculated leak intensity of the rock mass is also indicated at each bore-hole. The leak intensity has been calculated with an assumed hydraulic gradient of 1 and an inflow area of 32 m^2 per metre of the tunnel.

TABLE 5. Hydraulic conductivity and corresponding values of the leak intensity for the rock mass. The calculations are based on water tests in borings at the tunnel site.

	Mean values, whole bore-hole		Mean values, excluding surface rock		
Bore-hole no	Hydraulic conductivity m/s	Calculated leak intensity, l/min m	Hydraulic conductivity m/s	Calculated leak intensity, l/min m	Zones penetrated by the borings
D 61	$1.36 \cdot 10^{-6}$	2.53	$6.1 \cdot 10^{-7}$	1.13	D—E
D 62 A	$2.13 \cdot 10^{-7}$	0.40	$2.28 \cdot 10^{-7}$	0.42	K
D 63	$5.02 \cdot 10^{-7}$	0.93	$5.11 \cdot 10^{-7}$	0.95	G
D 64	$6.50 \cdot 10^{-7}$	1.21	$2.48 \cdot 10^{-7}$	0.45	E
D 66	$3.38 \cdot 10^{-7}$	0.63	$3.38 \cdot 10^{-7}$	0.63	F—G
D 67	$1.06 \cdot 10^{-6}$	1.98	$1.06 \cdot 10^{-6}$	1.98	H—I
D 68	$5.5 \cdot 10^{-7}$	1.02	$7.69 \cdot 10^{-8}$	0.14	E
Mean values	$6.68 \cdot 10^{-7}$	1.24	$4.4 \cdot 10^{-7}$	0.81	

AN ATTEMPT TO CALCULATE THE TOTAL WATER LEAKAGE INTO THE FORSMARK TUNNEL

On basis of the results of the geological and geophysical site exploration, we have tried to calculate the volume of the water leakages and the variations of the leak intensity along the tunnel line. The result of the calculation has been compared with and judged by the results of the geological survey in the tunnel.

DETERMINATION OF THE VOLUME OF THE LEAKAGE

If the values of the hydraulic conductivity for the bore-holes are known, the total water leakage into the tunnel can be calculated by certain mathematical relations. Here, the following relations according to Gustavsson *et al.* (1970), equation 4, or according to Wiberg (1961), equation 5, can be used:

$$Q = \pi kTL \tag{4}$$

or

$$Q = \frac{2\pi kTL}{\ln\left(T/R - \sqrt{(T/R)^2 - 1}\right)} \tag{5}$$

where Q = total leakage into the tunnel
k = hydraulic conductivity of the rock mass
T = depth below ground-water level
R = equivalence radius of the tunnel
L = total length of the tunnel

Generally speaking, equation (4) gives too large a value of Q but can be used in estimations with relative fair reliability. Equations (4) and (5) give the same answer for the leakage of a tunnel with the T/R ratio approximately equal to 4. For a tunnel with the T/R ratio equal to 10, equation (4) gives a value about 50 per cent larger than equation (5).

QUANTIFICATION OF THE TOTAL WATER LEAKAGE

One usually obtains information from the geophysical site exploration about the variation of the seismic velocity along a tunnel line and therefore it is possible to make a quantification from this parameter. However, the seismic velocity of a rock mass does not give a direct measure of its water-bearing capacity, though there is probably a certain synchronization between the seismic velocity and the water-bearing capacity. Zones of high seismic velocity and tight rock are probably mutually correspondent. There are at least two possibilities of interpreting a low velocity zone, either as a highly jointed, water-bearing, rock mass or as a highly jointed, rock mass sealed by clay alteration. In the latter case, the rock mass is usually fairly tight. In order to be able to make a division of the total inflow in spite of these uncertain factors, the assumption that there is a proportionate correlation between seismic velocity and water-bearing capacity must be valid.

For Swedish primary rocks of granitic and gneissic types, the seismic velocity ranges from about 3000 m/s for disintegrated rock to about 6000 m/s for sound and homogeneous rock. According to Bergman (1975), the water-bearing capacity ranges between 5000 l/min and 5 l/min for single zones of crushing and weakness. In a sound or lightly jointed rock, Eriksson (1975) has shown a variation ranging between 0.2 and 0.02 l/min and metre of tunnel. Normally, the quantity of leak water is considered to range between 50 and 0.05 l/min and metre of tunnel, if the extreme values are excluded. Consequently, the variation of the quantity of the leak water is considerably larger than the variation of the seismic velocity. This means that the condition is not linear but that the water-bearing capacity is proportional to some function of the seismic velocity. The following assumption permits of another quantification and a division of the total water leaking into a tunnel:

$$q = Kv^n \qquad (6)$$

where K = constant
q = water inflow
v = seismic velocity
n = exponent

This assumption means that the water inflow at each point along a tunnel is proportional to some exponential function of the seismic velocity at the same point.

From the above approximate variations of the seismic velocity, 3000 to 6000 m/s, and the corresponding water leakage, 50 to 0.05 l/min and metre, the exponent n in equation (6) can be determined approximately as –10. This exponent is not a constant but may vary in different areas with different geological conditions.

The hydraulic conductivity of a rock mass is generally determined from a number of bore-holes, usually located in zones of low seismic velocity. Therefore, it is reasonable to assume that the hydraulic conductivity of the rock mass and consequently also the total water inflow according to equation (5) will have too high values in comparison with the conditions in the tunnel as a whole. This difference may correspond to the difference in seismic velocity between the tunnel as a whole and that part of the rock which has been penetrated by the bore-holes. On condition that the assumption according to equation (6) is applied a new value of the total water inflow can be calculated according to equations (7) and (8):

$$Q_v = Q \left(\frac{V}{\bar{v}_b}\right)^{-10} \qquad (7)$$

After reduction,

$$Q_v = Q \left(\frac{\bar{v}_b}{V}\right)^{10} \qquad (8)$$

where Q_v = the total inflow into a tunnel quantified according to the seismic velocity

Q = the total inflow according to equation (5)

$\bar{v}_b$ = the mean value of the seismic velocity of the rock mass which has been penetrated by the bore-holes (used for tests of water loss)

V = the mean value of the seismic velocity of the whole tunnel line

A more correct representation of the volume of water leakage may be derived from equation (8), in comparison with the value of Q, which does not take the seismic velocity into consideration.

Now, it is interesting to know how the water leakage is going to vary as a function of the tunnel section excavated and to know when a greater intensity of water leakage can be expected. An evaluation of these conditions must be made if the relative water inflow of each seismic interval is to be calculated. By comparing the amount of these relative values of water inflow with the total water inflow according to equation (8), we may get an idea of the variation of the water inflow along the tunnel line. The values of the water inflow of the individual seismic zones can be used to calculate the leak intensity and the increase as a function of the tunnel section excavated. This means that the increase of the total volume of the water leakage within a seismic zone is linearly related to the length of the zone. The slope of the linear function is determined by the ratio between the measured seismic velocity within the zone and the mean value of the seismic velocity along the tunnel line.

CALCULATION OF TOTAL WATER LEAKAGE

Using the results of the geological and geophysical exploration, a calculation of the water leakage into the Forsmark tunnel can be made. The calculated values of the hydraulic conductivity are summarized in Table 5 and the seismic velocity in Fig. 3 and in Fig. 16. With the following values inserted in equation (5), the total water leakage can be calculated:

$T=30$ m for $L=440$ m
$T=60$ m for $L=1050$ m
$T=30$ m for $L=431$ m
$R=4$ m
$Q=1232+4680+1208=7120$ l/m

The mean value of the seismic velocity of the whole tunnel line is 5035 m/s, whereas the mean value of the rock mass at the bore-holes is 4800 m/s. A new value of the water leakage with regard to the variations of the seismic velocity can now be calculated from equation (8):

$$Q=7120 \cdot \left(\frac{4800}{5035}\right)^{10} = 4415 \text{ l/min}$$

This Q-value is the total quantity of water that can be expected to leak into the tunnel. It is now possible to divide this total leakage between the seismic units. On the basis of this division, it is possible to make a calculation of the leak intensities. The result is graphically shown in Fig. 17, where the histogram represents the expected leak intensities of the units. The cumulative curve shows how the total quantity of the water leakage can be expected to increase as a function of the excavated tunnel length.

REAL CONDITIONS OF THE WATER LEAKAGE

The total quantity of the water leakage into the Forsmark tunnel is 3000 l/min. It can be divided between the ten different rock-mechanically conditioned zones, zones (A–K in Fig. 3). The leak intensities in the zones are shown by the histogram in Fig. 18.

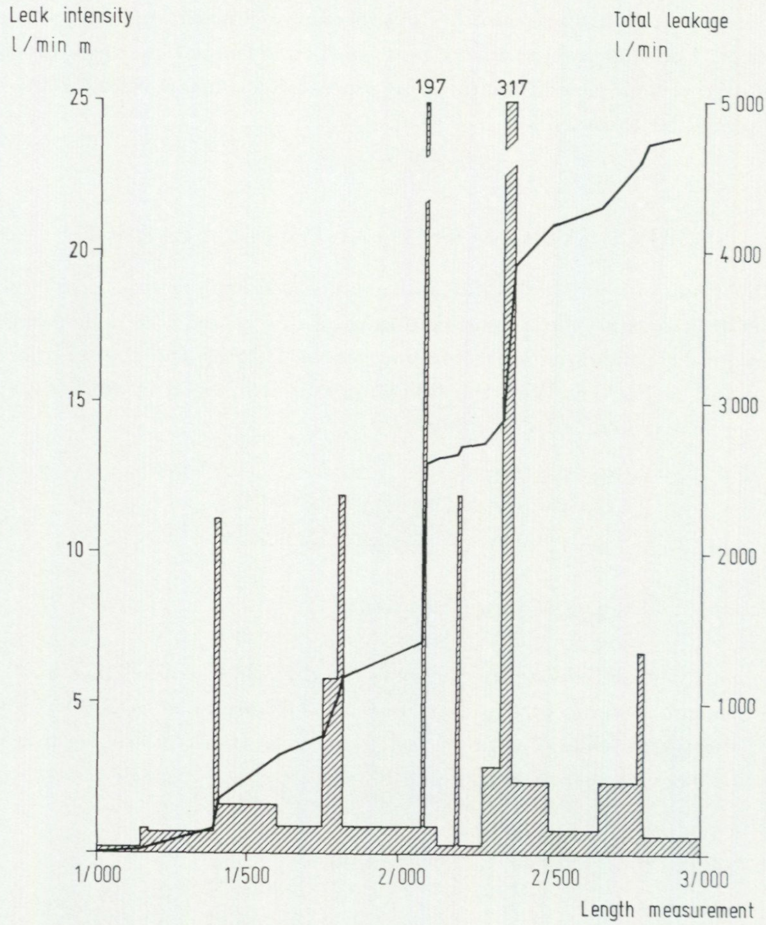

Fig. 17. Expected water leakage into the tunnel, calculated from the geological and geophysical site exploration. The histogram represents the expected leak intensities of the different seismic velocities and the cumulative curve shows the expected total quantity of water leakage as a function of the excavated tunnel section. The leak intensity is given in litres per minute and metre of tunnel (l/min m).
Läckageberäkning baserad på utförda förundersökningar. Histogrammet visar den beräknade läckageintensiteten för varje seismiskt hastighetsintervall och den heldragna kurvan visar den totala inläckningen som funktion av utsprängd tunnellängd. Läckageintensiteten anges i liter per minut och meter tunnel (l/min m).

The pre-grouting which was done during the tunnelling probably reduced the water leakage into these sections. The real effect of the pre-grouting could not be determined, as no continuous measurements of the leakage have been made. The positions of the grouted sections and the consumption of cement on each occasion of grouting are shown in Fig. 11.

From a general point of view, all the larger water leakages can be assigned to

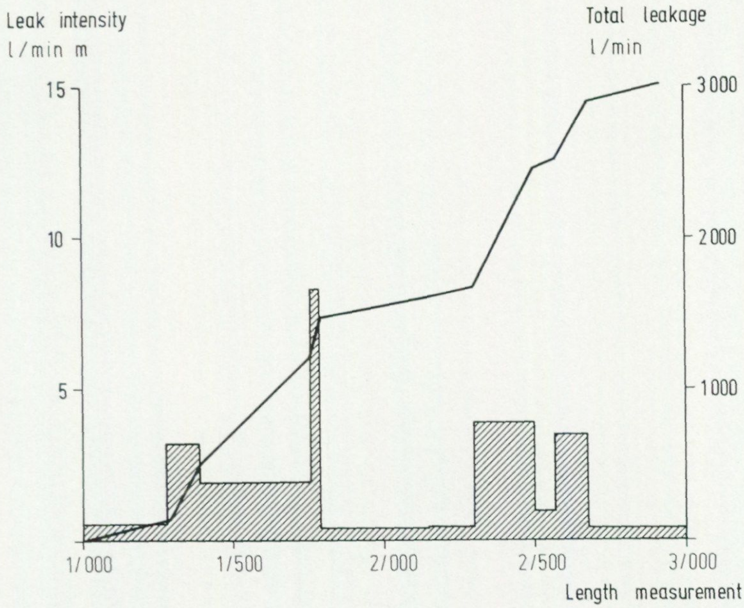

Fig. 18. Real volume of the water leakage, based on the observations and measurements in the tunnel. The histogram represents the leak intensities within the ten rock-mechanical zones and the cumulative curve shows the cumulative effect as a function of the excavated tunnel section. The leak intensity is given in litres per minute and metre of tunnel (l/min m).
Verklig inläckning baserad på de utförda observationerna. Histogrammet visar läckageintensiteten i de tio bergmekaniskt betingade zonerna och den heldragna kurvan den kumulativa effekten som funktion av utsprängd tunnellängd. Läckageintensiteten anges i liter per minut och meter tunnel (l/min m).

the four zones of weakness in the tunnel. A curve which describes the increase of the volume of water leakage as a function of the excavated tunnel length has been constructed on the basis of the intensity of the leakage in the zones. This curve is to be found in Fig. 18.

THE RESULT OF THE CALCULATION

The calculated volume of water leakage exceeds the real, measured volume by about 50 per cent. The reason for the difference is to be found in several conditions discussed in the following section.

A comparison between the intensities of the leakage in the seismic zones and the ten rock-mechanical zones shows a fairly good correspondence. However, there are a number of zones in the calculation with very high leak intensities which do not have any correspondences in the tunnel. The total water leakages according to the calculation and according to the real result as a function of the excavated tunnel

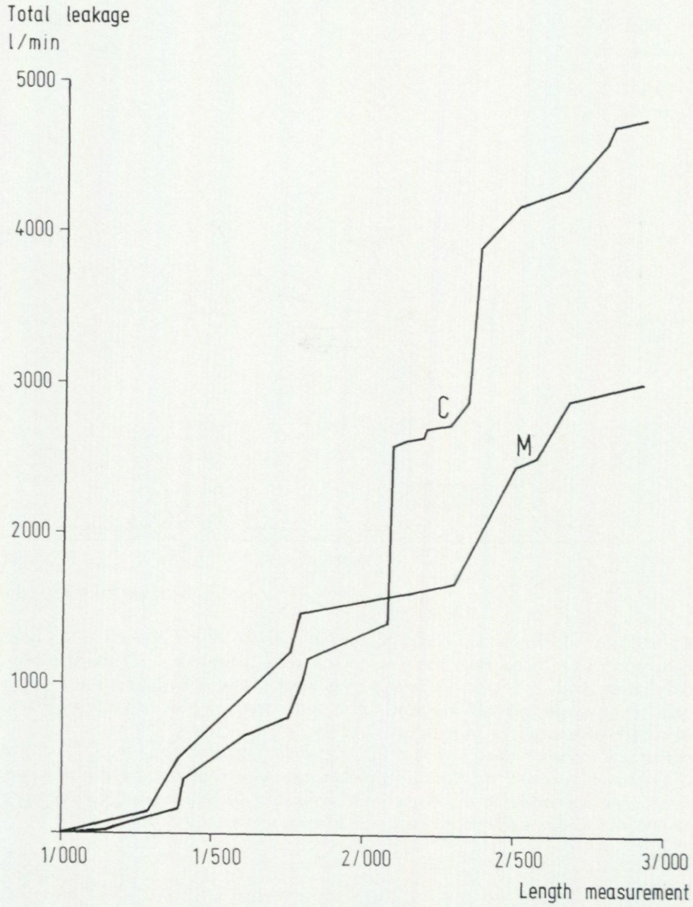

Fig. 19. Comparison between the calculated and the real total volumes of the water leakage
Jämförelse mellan den beräknade och den verkliga totala inläckningen

section in Fig. 19 are in fairly good agreement. Steeply inclined sections in the calculated diagram generally correspond to similar sections in the real curve. However, in the calculation there are curve sections with high gradients with no correspondences to the real curve.

DISCUSSION

The reason for the difference between the calculated leakage and the real result is to be found in a number of different conditions. It has already been pointed out that the seismic velocity alone is not a certain measure of the water-bearing capacity of a rock mass.

Zones of clay-fillings may be found connecting onto zones of weakness in the rock mass, for example, zones of crushing and jointing. These zones of clay-fillings may have a considerable lowering effect on the water-bearing capacity of the rock mass (Ahlberg and Lundgren 1975). Also other forms of alteration, for example, chlorite fillings, may effect a reduction of the hydraulic conductivity of the rock mass. The orientation of the tunnel is also of great importance.

The seismic velocity is dependent on the direction of the profile in relation to the structure in rocks with plane-parallel structures like the paragneiss in the Forsmark tunnel. Generally, the seismic velocity is higher parallel to the structure than transversely to it. As mentioned above, the comparison between the seismic velocity and the leak intensity (Fig. 16) shows a fairly good correlation in the four zones of weakness. The correlation in two of the zones is asymmetrical in relation to the direction of the tunnel. However, this corresponds to the dip of these zones. In some cases, the zones of low seismic velocity do not correspond to any deterioration in the quality of the rock mass or to any noticeable volume of water leaking into the tunnel. Probably, the exponent n in equation (6) is not a constant but a function of the seismic velocity, the water-bearing capacity and an unknown number of geological and hydraulic parameters. This condition leads to an additional uncertain factor which influences the calculated quantity of the water leakage. These conditions are also valid for equation (6) in general.

Naturally, all these factors affect the calculation of the leakage, as the calculation is based on the fact that the water-bearing capacity varies with the seismic velocity. Generally speaking, it has been established that the calculated value of the water-bearing capacity tends to be larger than the real result, as most parameters overestimate the water-bearing capacity of the rock. Examples of such overestimating parameters are clay alteration and pre-grouting. Here, the tectonic pattern is of great importance. Tension zones often include open joints, while shear zones are usually tight, depending on the state of strain of the rock mass. The behaviour of the rock mass during a tectonic phase, i.e. the disposition to disintegration and clay alteration, is of great importance as regards the water-bearing capacity of the zones of weakness. The reduction of the total, real, water leakage caused by the pre-grouting also contributed to an increase of the difference between the calculation and the real result.

CONCLUSION

The difference in total leakage between the calculated and the observed values is here about 50 per cent. Considering the difficulties in determining the parameters that are of decisive importance as regards the water-bearing capacity of the rock mass, this difference may be considered to be acceptable. For the present, there is no exact method of determining the quantity of water leaking into tunnels, so most of the predictions must be quite uncertain. In these circumstances, the method of quantifying the results of geological and geophysical explorations described here may satisfy a certain want. The method is marred by obvious shortcomings and the degree of truth in the assumptions made may vary within very wide limits. It is also necessary to apply the method to a large number of objects, in order to improve the reliability.

SAMMANFATTNING

I samband med den geologiska karteringen av Forsmarkstunneln har en särskild undersökning av tunnels vattenläckage utförts. Avsikten med detta arbete är i första hand att försöka dokumentera vattenläckagens uppträdande och storlek i relation till de geologiska och tektoniska förhållandena. Avsikten är också att ge en bild av hur berggrundens olika vattenmagasin kommunicerar sinsemellan och med havsvattnet.

Berggrunden längs tunnellinjen består i huvudsak av gnejsgranit och sedimentgnejs. I dessa båda huvudbergarter finns gångar och massiv av pegmatit och grönsten. I en cirka 200 meter lång zon utgörs bergarten av en breccierad gnejsgranit med talrika genomådringar av kvarts och kalcit. I denna zon finns ett antal hydrotermala gångar och lerfyllda sprickor. Tunneln skär med förhållandevis gynnsam vinkel fyra väl markerade svaghetszoner av varierande bredd.

Sprickbilden för de båda huvudbergarterna skiljer sig genom att sprickplanen i sedimentgnejsen i allmänhet överensstämmer med bergartens skiktplan, under det att gnejsgraniten uppvisar en förklyftning, som är mer oberoende av bergsstrukturen.

Bergspänningsmätningar är utförda på fyra ställen i tunneln för att erhålla kännedom om bergets spänningstillstånd. De högsta tryckspänningarna återfinns samliga i gnejsgraniten. Den regionala bilden av spänningsfördelningen i berggrunden ger en högsta tryckspänning i riktningen N 45° V, som är ett medelvärde för samtliga mätningar.

Vattnets allmänna uppträdande i relation till bergmassans olika spricksystem och tektoniska förutsättningar tycks följa vissa bestämda mönster, vilket har medgivit en klassificering av läckagens uppträdande i nedanstående fem huvudgrupper:

1. Vatteninläckningen är koncentrerad till hål eller lokala vidgningar av spricköppningen i en i övrigt tät spricka. Förhållandet gäller framför allt flacka sprickor i gnejsgraniten.
2. Vattnet uppträder längs flacka eller medelbranta sprickplan ofta som distinkta flöden men med avsaknad av markerade öppningar.
3. Inläckningen sker längs branta sprickplan i allmänhet som distinkta flöden vid tunnelns sula eller vid sprickans nedre begränsning.
4. Vattenläckaget är distinkt och härrör från korspunkter mellan två eller flera sprickor. Sprickorna i sig själva är i övrigt täta eller medger en mycket begränsad inläckning.
5. Läckaget kan ej hänföras till någon speciell spricka eller sprickgrupp, utan vattnet läcker in på bred front som ett diffust flöde.

Av dessa fem grupper har grupp 1 och 4 högre vattenföring än de övriga beroende på, att dessa båda lokalt har en kraftigt ökad sprickvidd. Totalt sett ger grupp 4 den högsta inläckningen medan grupp 3 har den lägsta. Läckageuppträdandet enligt grupp 3 har därtill ofta ett med tiden minskande läckage. De fyra tektoniska svaghetszonerna svarar

för den högsta totala inläckningen. Cirka 60 procent kommer från dessa zoner. Områdena däremellan är till stora delar helt torra. Detta trots tunnelns gynnsamma läge med tillgång till ett stort infiltrationsmagasin. En klar skillnad mellan vattnets uppträdande och läckageintensiteten mellan tunnelns olika huvudbergarter kan iakttas. Vattenläckagen i gnejsgraniten är större och uthålligare, medan läckagen i sedimentgnejsen är små och ofta uppvisar en med tiden minskad intensitet. Detta förhållande hänger samman med sprickbilden, där gnejsgranitens horisontella sprickor skär igenom strukturen och öppnar en förbindelse med omgivande vattenmagasin.

I samband med tunnelkarteringen uttogs och analyserades tio vattenprover och ett referensprov av havsvattnet. Allmänt kan sägas att det föreligger stora skillnader mellan de olika proverna från tunneln och mellan läckvattnet och referensprovet. Förstärkningsarbeten i form av injektering, sprutbetong och bergbultning har troligtvis förorsakat en ändring av läckvattnets kemiska sammansättning. Den största störningskällan torde vara den förinjektering, som utfördes i samband med tunneldrivningen. De vattenprover som är tagna i eller i närheten av förinjekterade partier uppvisar anmärkningsvärd hög totalhårdhet i jämförelse med prover från oinjekterade partier. Totalhårdheten är dock hög för samliga läckvattenprover. Den kanske mest anmärkningsvärda skillnaden mellan havsvattnet och läckvattnet gäller pH-värdet, som för läckvattnet är betydligt lägre än för havsvattnet. Vad gäller järn-, ammonium- och fluoridhalten kan allmänt sägas att den är betydligt högre för läckvattnet. Kloridhalten är i läckvattnet i allmänhet något högre än för referensprovet. I ett läckvattenprov är dock kloridhalten cirka 50 procent högre. En jämförelse mellan de olika kvävejonerna tyder på, att kvävet är mer oxiderat i havsvattnet än i läckvattnet. Variationerna i nitrit- och nitrathalterna har troligtvis förorsakats av spränggaserna i samband med tunneldrivningen.

Två av läckvattnet avlagrade sedimentprover har analyserats. Innehållet av organiskt material och bundet vatten i de båda proverna ligger på cirka 20 procent. Järnhalten är mycket hög i de båda proverna och manganhalten är nio gånger större i det ena provet.

Ett försök till korrelation har gjorts mellan den seismiska gånghastigheten längs tunnellinjen och bergets vattengenomsläpplighet. Överensstämmelsen mellan parametrarna i svaghetszonerna är förhållandevis goda. Vissa av de vid undersökningen registrerade låghastighetszonerna motsvaras inte av någon ökad vatteninläckning i tunneln, och några geologiska indikationer kunde inte heller upptäckas vid tunnelkarteringen, som skulle kunna förklara dessa låghastighetszoner. De lerzoner som uppträder kan också verka tätande på berget och därmed nedsätta den totala vatteninläckningen till tunneln.

Med utgångspunkt från de systematiska vattenförlustmätningar, som utförts i borrhålen längs tunnellinjen, har bergets permeabilitet beräknats till $6.7 \cdot 10^{-7}$ m/s som ett medelvärde för samtliga mätningar.

Med kännedom om bergets permeabilitet, seismisk gånghastighet och de olika tunnelparametrarna såsom tunnelarea, bergtäckning och vattentryck har ett försök gjorts till beräkning av den totala vatteninläckningen till Forsmarktunneln. Utfallet av beräkningen har sedan bedömts utifrån de faktiska förhållanden, som framkommit under den byggnadsgeologiska karteringen. Den skillnad i totalinläckning mellan beräknad och verklig inläckning som vi har för Forsmarktunneln är av storleksordningen 50 procent. Generellt kan konstateras att det beräknade värdet på inläckningen tenderar att ligga högre än det verkliga utfallet, eftersom låghastighetszonerna ofta innehåller tätande material. Här har även den tektoniska bilden stor betydelse. Den minskning av den totala verkliga inläckningen, som orsakats av de utförda förinjekteringarna har även bidragit till en ökning av skillnaden mellan beräkning och verkligt utfall.

ACKNOWLEDGEMENTS

To Drs Jan De Geer and Jüri Martna, we wish to express our sincere appreciation of their continued help as critics and advisors.

Our thanks are due to Mr. K. A. Scherman, Chief Engineer at the Swedish State Power Board in Stockholm, for his encouragement and great support during our work.

We also wish to express our thanks to Mr. Oskar Rinne, Project Manager at the Swedish State Power Board at Forsmark, for his full support during our field work.

Dr Jüri Martna and Mr. K. A. Scherman (Swedish State Power Board) and Drs Jan De Geer, Åke Möller, Gösta Persson and Göran Stålhös (Geological Survey of Sweden) have read and criticized the manuscript.

We are very grateful to all these persons and to our other colleagues at the Swedish State Power Board at Forsmark and Stockholm and at the Geological Survey of Sweden.

Mr. Neil Tomkinson has corrected the English.

REFERENCES

BeFo = Stiftelsen Bergteknisk Forskning (Swedish Rock Mechanics research foundation), Stockholm.

BFR = Statens råd för byggnadsforskning (National Swedish Building Research), Stockholm.

GFF = Geologiska Föreningens i Stockholm Förhandlingar (The Transactions of the Geological Society of Sweden), Stockholm.

ISRM = International Society for Rock Mechanics.

SGI = Statens Geotekniska Institut (Swedish Geotechnical Institute), Linköping.

SGU = Sveriges geologiska undersökning (Geological Survey of Sweden), Stockholm.

Ahlberg, P., and Lundgren, T., 1975: Grundvattensänkning till följd av tunnelsprängning. — SGI-Publikation, Proj. Nos. 20122 and 20400, 52 pp. Linköping.

Banks, D. C., 1972: In situ measurements of permeability in basalt. Proceedings, Symposium on Percolation through Fissured Rock. Section TI-A. — ISRM, p. 1—6. Stuttgart.

Bergman, M., 1975: Grundvatteninläckning i bergrum och tunnlar. Inventering och sammanställning av läckvattenmängder. — Seminarium om geohydrologisk undersökningsmetodik, May 21st, 1975. BFR, p. 33—46. Göteborg.

Carlsson, A., and Olsson, T., 1976a: Forsmark kraftstation. Geologisk kartering, kylvattentunnel. — Internal report. Statens Vattenfallsverk, 8 pp. Stockholm.

— 1976b: Bestämning av berggrundens permeabilitet genom vattenförlustmätning. — Vannet i Norden, nr 3, Vol. 9, p. 29—35. Oslo.

Ehrenborg, J., and Stephansson, O., 1976: Sprickor i Uppland sedda från satellit. — Forskning och Framsteg, nr 6, p. 45—35. Stockholm.

Eriksson, A., 1975: Grundvatteninläckning i bergtunnlar. — Seminarium om geohydrologisk undersökningsmetodik, May 21st, 1975. BFR, p. 1—32. Göteborg.

Gillberg, G., 1967: Distribution of different limestone material in till. — GFF 89, p. 401—409. Stockholm.

Gustavsson, Y., Sund, B., and Lindh, A., 1970: Grundvattensänkning vid tunneldrivning. — Byggmästaren, nr 6, Vol. 49, p. 23—26. Stockholm.

Hagerman, T., 1956: Byggen, berggrund och grundvatten. — Teknisk Tidskrift, p. 799—804. Stockholm.

Hiltscher, R., 1976: Forsmark kraftstation, block 1 och 2. Mätning av bergets initialspänningar i avloppstunneln. — Internal report. Statens Vattenfallsverk, 7 pp. Stockholm.

HILTSCHER, R., and STRINDELL, L., 1976: Bergspänningsmätningar som underlag vid projektering av stora bergrum. English Summary: Rock stress measurements in connection with the design of large underground openings. — BeFo Bergmekanikdag 1976, p. 151—158. Stockholm.

LARSSON, W., 1973: Forsmark kraftstation, aggr. 1 och 2, avloppstunneln: Berggeologiska förhållanden efter tunnellinjen. — Internal report. Statens Vattenfallsverk, 6 pp. Stockholm.

LOMIZE, G. M., 1951: Water flow in jointed rocks (in Russian). — Gosenergoizdat.

LOUIS, C., 1967: Strömungsvorgänge in klüftigen Medien und ihre Wirkung auf die Standsicherheit von Bauwerken und Böschungen im Fels. — Doctoral thesis, Univ. Karlsruhe. O. Berenz, 121 pp. Karlsruhe.

MOBERG, M., 1974: Forsmark kraftstation, aggr. 1 och 2. Avloppstunneln. Grundundersökningar 1971—1973. — Internal report. Statens Vattenfallsverk. Stockholm.

MOYE, D. G., 1967: Diamond drilling for foundation exploration. — Civil Engineering Transactions, Vol. CE 9, No. 1, p. 95—100. Sydney.

MÖLLER, Å., ENGQVIST, P., and MÜLLERN, C.-F., 1976: Hydrogeologiska förhållanden inom Närkeslättens sedimentära berggrund. — SGU C 721, 64 pp. Stockholm.

PALMQVIST, K., 1975: Grundvatten och tektonik. Erfarenheter från några olika beranläggningar. — Seminarium om grundvatten i berg, Dec. 6th, 1974. BFR, p. 36—51. Göteborg.

WENNER, C.-G., 1951: Grundvattenförhållanden i södra Sveriges berggrund. — Teknisk Tidskrift, Vol. 47, p. 1—6. Stockholm.

WIBERG, L., 1961: Grundvattenströmning till rörledningar. — Doctoral thesis, Kungl. Tekn. Högskolan, 86 pp. Stockholm.

PRISKLASS D

Distribueras genom
LiberKartor
162 89 VÄLLINGBY

Schmidts Boktryckeri AB
Helsingborg 1977

ISBN 91-7158-125-1